ABSTRACT

MOHAN KRISHNAN, ARCHANA. Robust Pressure of Meta-Stable Textile Fabrics. (Under the direction of Dr. Hoon Joo Lee.)

Recent developments in the dynamic world of self-cleaning surfaces point at the growing pace of superoleophobic fabrics. One of the important properties that such fabrics possess is the re-entrant nature which allows a liquid drop under pressure to be pushed back to the top of the surface after pressure release without a wet interface. The maximum pressure that causes penetration of the drop is the robust breakthrough pressure. Robustness is the ability of a fabric to push a liquid drop that has been forced into the structure back up to the surface. A meta-stable surface is capable of transcending between wetting and dewetting regimes due to the small energy barrier separating them. Low surface tension liquids exhibit this property.

Presently, there is no method to quantify the pressure that a fabric can withstand before liquid drop penetration occurs. Hydrostatic pressure testing is the golden standard that is used for testing penetration of liquids through fabrics, but this test becomes void for small droplets that are insignificantly affected by gravity and that tend to spread initially rather than penetrate. Previous literature points at a qualitative measure for predicting the robust breakthrough pressure.

This research focuses on quantifying the robust pressure to observe the wetting of a superoleophobic fabric whose principle identity is complete non-wetting by liquid. This has been achieved by developing the “robustometer”. This instrument can measure the pressure

that causes spreading of drops before penetration and determines if the fabric is wet or dewet after pressure removal. The first effort at development involved construction of the device, testing of fabrics, and identifying shortcomings. The most important of the limitations that adversely affect pressure measurements is the sagging of the fabric surface. The demerits can be eliminated by small improvisations.

Test runs on the robustometer have proved that a 10 µl droplet of liquid when subjected to external pressure spreads over a fabric surface forming a thin film before penetrating into the structure. The pressure required to trigger spreading and imbibitions is smaller than the predicted breakthrough robust pressure. This is of prime importance while testing functional fabrics that protect against penetration by toxic substances that are lethal at volumes of 1 µl.

Robust Pressure of Meta-Stable Textile Fabrics

by
Archana Mohan Krishnan

A thesis submitted to the Graduate Faculty of
North Carolina State University
in partial fulfillment of the
requirements for the degree of
Master of Science

Textiles

Raleigh, North Carolina

03/16/2011

APPROVED BY:

_____
Dr. Hoon Joo Lee
(Chair of Advisory Committee)

_____
Dr. Stephen Michielsen
(Member of the Advisory Committee)

_____
Dr. Abdel-Fattah Seyam
(Member of the Advisory Committee)

DEDICATION

To

My

Dearest

Mum & Dad

BIOGRAPHY

Archana Mohan Krishnan received her Bachelor of Technology in Textile Technology from Anna University, India in 2009. She entered the Master of Science program in Textiles at the Department of Textile Apparel & Technology Management, North Carolina State University in fall 2009. She is currently fulfilling her requirements to obtain her graduate degree. On completion of her degree, she plans on pursuing a career in the textile industry in the area of functional product development.

ACKNOWLEDGEMENTS

This work is supported by a contract from the Defense Threat Reduction Agency (DTRA), under contract HDTRA 1-08-1-0049.

I would like to offer my sincere gratitude to my mentor and advisor, Dr. Hoon Joo Lee for bestowing me with one of my best opportunities and helping me through my graduate years, offering courage and support all the way. This work was made possible by her encouragement and unwavering belief in my ability.

I wish to address a very special “thank you” to Dr. Stephen Michielsen, one of the most knowledgeable persons I have had the good fortune to cross paths with. His invaluable advice and guidance paved the way for this work and helped sustain it till the very end.

I would like to express sincere thanks to Dr. Abdel-Fattah Seyam for being on my committee and helping me with my final defense and Dr. Nancy Cassill for providing me with much-needed encouragement on my first day of class.

I would also like to acknowledge Mr. Robert Cooper for answering my constant flow of questions over the two years.

I wish to acknowledge my fellow team members, Rahul Saraf, Jinlin Zhang, Priscilla Tan, and Dr. Jinmei Du who helped me immensely and offered support at various stages of this work, personally and professionally. Yongxin Wang deserves special mention for her dedication in helping me refine and successfully conclude this thesis.

I especially thank my friends Dnyanada Satam, Ravikanth Vangala, and Balaji Sundaravel for their encouragement and support. Special thanks to Arul for being there through thick and thin.

Last but not the least, I offer my heartfelt appreciation to my beloved parents and brother who push me onto bigger and better things. I love you.

TABLE OF CONTENTS

LIST OF FIGURES

LIST OF TABLES

Chapter 1 Introduction

With increasing commercial interest in the phenomenal area of material science, there has been profound research in the area of self-cleaning textile surfaces. Since the first observation[1] made on the versatility of the Lotus leaf's self-cleaning ability[2], there has been a spurt in mimicking this phenomenon for diverse technological applications such as self-cleaning window panes, stain-free apparel, protective textile surfaces, especially in military, environment protection, etc. This, in turn has led to in-depth analysis of the mechanisms involved in the propagation of an oil-drop on geometrically as well as chemically modified surfaces.

The term hydrophobic is used to describe the wetting of a solid surface by water, while oleophobic is used to describe the wetting behavior of oils. Superoleophobicity is defined as the state at which a specified liquid drop exhibits contact angles greater than 150º on a textured surface with protrusions[3]. Protrusion is a roughness feature that has height, width, tip, and radius of curvature. Scale-dependent protrusions are true causes of high liquid contact angles. The contact angle hysteresis, which is the difference between the advancing and receding contact angles does not have to be very small (less than 5°) for this phenomenon as the surface would remain dewet by the sessile droplet at high contact angles in any case.[4]

1.1. Purpose of this study

It has been established that superhydrophobic and superoleophobic surfaces are developed based on surface roughness and surface tension.[5] Since liquids like dodecane (25 mN/m) and Kaydol (31 mN/m) have very low surface energies, repellency cannot be obtained as easily as with water (72.8 mN/m). In such cases, rough omniphobic surfaces need to be developed using a third parameter: robustness, which is defined as the capability of a fabric structure to retain its inherent structure and property against deformations and interactions with liquid droplets applied at mechanical pressures. This robustness is particularly in context to superoleophobicity. Superoleophobicity is the property of a surface to exhibit static contact > 150° with oil.[6]

Presently, there is no published work on quantitatively analyzing the robust breakthrough pressure. This research deals with the robustness of fabrics wherein an instrument to practically measure the robustness of a fabric was developed and the fabrics on which robustness was tested were characterized with reference to the superhydrophobic dewet state.

The goal is to be able to measure the robustness of a fabric against different pressures and liquids. Robustness is an essential criterion for superoleophobicity. This involves a comprehensive study of the basic Wenzel [7] and Cassie-Baxter[8] models to study robust superoleophobic surfaces. Such surfaces can be best described by a meta-stable Cassie-Baxter model which is consistent with the Cassie-Baxter structure at a local minimum of free energy with the Wenzel state at a global minimum of free energy as established by Marmur.[9]

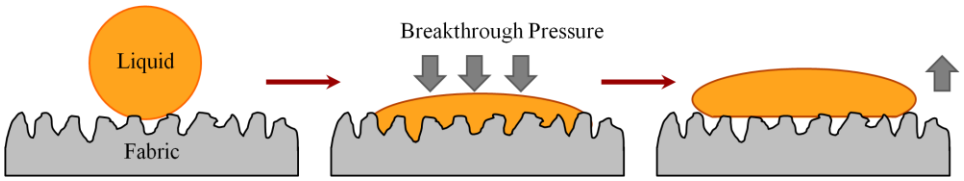

Figure 1.1. Demonstration of robust pressure- A liquid droplet is being pushed into the inner-protrusion space of an oleophobic fabric to the wetting regime by defeating the suspension force, but on removal of pressure, it returns to the meta-stable Cassie-Baxter state.

This is an intermediate region during the transition from the non-wetting heterogeneous interface to a fully-wetted homogeneous regime. This state is a stable composite before the eventual Wenzel manifestation.

1.2. Significance of this study

The importance of robustness rises from the fact that textile surfaces are rough. Hence, the stability of hydrophobic, oleophobic fabrics is dependent on the surface chemistry and roughness features. The pressure acting on the surface of a fabric determines the ease with which a liquid drop can pass through it. The ability of the fabric to push the drop back to the surface to be shed or wiped away is a phenomenon that can find use in various applications such as performance wear, military, medical, and home furnishings. This ability is usually achieved on superhydrophobic and superoleophobic surfaces roughened by chemical and topographical modifications of the surface. Robustness is necessary to indicate if a drop transitions from the Cassie-Baxter state to the Wenzel state as this has a direct implication on the credibility of the design of a rough surface.

The hydrostatic pressure testing is the golden standard method for testing the repellency of liquids by high performance fabrics. The pressures applied in these tests are large enough to cause permeation of large volumes of liquids through the fabric surfaces. Hence, when minute droplets of fluid are involved, the hydrostatic pressure test proves to be ineffective as the influence of gravity on drops as small as 1µl is insignificantly small. Besides, such small drops do not penetrate the fabric under pressure, but are more likely to spread along the surface before imbibition. This could be a revelation in the testing of surgical wear in medical textiles wherein, hydrostatic pressure tests are carried out for testing the penetration by blood and other body fluids. Although, blood pressures in the operating rooms are very high, the dispersed droplets on impact with clothing are small enough to spread rather than penetrate the protective clothing even at high rates of impaction. This can be resolved by the robustness test studied in this research. It describes the wetting behavior of small drops under mechanical pressure.

Chapter 2 Literature Review

This research is based on the wetting of high liquid shedding properties of treated textile surfaces. The production of such fabrics is studied to understand the hierarchical structure of the surfaces influencing liquid behavior. The stability of fabrics under the influence of external pressure is reviewed along with the conditions of a liquid in a meta-stable free energy state.

2.1. Research background

The ideology of roughness-induced surfaces has existed since 1936 when Wenzel discovered that contact angle of a liquid was different on a rough surface than on a smooth surface of similar composition. Cassie and Baxter[8] introduced the idea of a composite interface with liquid drops being supported on a porous solid surface, supported partly by air cavities with contact angles of 180º. This solid-liquid-vapor interface was an oddity as compared to the complete homogeneously wet solid-liquid regime. Shuttleworth and Bailey[26] studied the spreading of a liquid over a rough solid and proved that the contact angles at the minimum of surface energy agreed with the values predicted by Wenzel and Cassie-Baxter. Johnson and Dettre[27] observed that the completely wet homogeneous state and the heterogeneous Cassie-Baxter state corresponded to the two meta-stable phases of a droplet. Research in the field of wetting gained momentum with the realization of the "Lotus-Effect" with its self-cleaning phenomenon which is of great technological importance.[1] Further studies were done on the

metastability of the drops on artificial superhydrophobic surfaces and it was pointed out that the existence of the homogeneous or heterogeneous interfaces depended on the method of application of the droplet and the morphology of the surface roughness.[28,9, 29,21] Marmur[9] obtained the conditions for when transitions take place between the homogeneous and heterogeneous interfaces. Patankar[29] pointed out there are multiple equilibrium meta-stable phases to which the drop might transition to which correspond to respective local minima in free energy. The state that the drop comes to rest in will not necessarily have the lowest energy, rather it would settle in an intermediate meta-stable region without wetting the substrate[21]. He also showed that the shape of the drop depends on the formation of the drop. Extrand[30] pointed out that the determination of the Wenzel or Cassie-Baxter regime also depends on the droplet size, due to the gravitational effect. But, this particular factor has been eliminated in this research as in almost all cases droplets as small as 10 µl are used. The effect of gravity on such small-sized drops is insignificant. It was observed that dual roughness patterns on superimposed surfaces[23, 31], self-affined structures[32], and fractal roughness[33] contributed towards superhydrophobicity. Herminghaus also pointed out that such self-affined roughness even supported liquids with low surface tensions when local equilibrium conditions are satisfied for meta-stable states. Lafuma and Quéré[28] suggested that based on contact angles and drop size, Cassie-Baxter and Wenzel transitions can be determined and this would in turn aid in achieving a robust anti-wetting state. We know that when a drop is pressed, as in the robustness experiments in this research, the contact angles change dynamically in agreement with Bico et al.[34] who observed that the contact angles

decrease as impalement of the fabric structure occurs by the liquid under pressure. Burton and Bhushan[35] studied that roughening a hydrophilic smooth surface, decreases the contact angle of a drop, while similar effects on a hydrophobic surface would increase the contact angle. These findings were in agreement with observations made on plants with similar hydrophilic and hydrophobic rough surfaces.[36]

A number of surfaces in nature use extreme water repellency for specific purposes; be it water striding or self cleaning. A number of surfaces encountered in nature are superhydrophobic, displaying water (surface tension γ =72.8 mN/m) contact angles >150°, and low contact angle hysteresis. The most widely-known example of a superhydrophobic surface found in nature is the surface of the lotus leaf. It is textured with small 10-20 micron sized protruding nubs which are further covered with nanometer size epicuticular wax crystalloids.[1] In the last decade, scientists have studied plants in nature with a rough surface to understand the lyophobic effect in depth.[1, 37] The plants focused on in these studies were the Lotus (*Nelumbo nucifera*) and Taro (*Colocasia esculenta*) rough leaves.

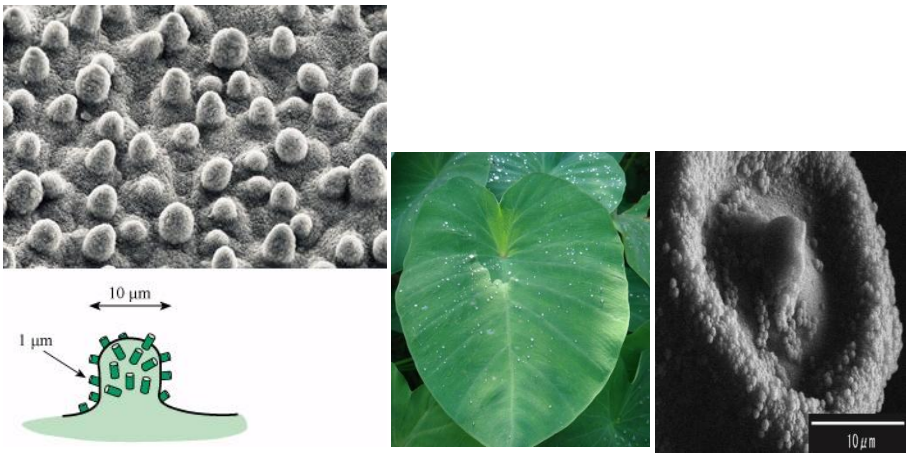

Figure 2.1. SEM images of the otus leaf (left) and Taro leaf (right) microscopic structures.[38]

The lotus leaf has bumps on its surface which are covered by an epicuticular waxy layer as is shown in Figure 2.1. This waxy layer made of hydrocarbons is hydrophobic with water contact angles of 95°-110°. It is the bumps that enhance the contact angle as seen in a Wenzel rough surface. The static contact measured on the surface was 160°. The ease with which the drops roll-off indicates that the surface has low hysteresis which hints at the underlying air pockets indicating a Cassie regime.[1, 39] Numerous studies have shown that it is this combination of surface chemistry plus roughness on multiple scales (micron and nanoscale) that imbues superhydrophobic character to the lotus leaf surface. The effects of surface chemistry and surface texture can be controlled to create high levels of oil-repellency and superoleophobic behavior.

Lafuma and Quéré[28] observed that compressing a liquid drop under adequate pressure induces Wenzel or the completely wet state, wherein the degree of adhesion is dramatically

enhanced as the liquid is forced to follow the texture of the surface. This is in stark contrast to the Cassie-Baxter state which has a lower contact angle hysteresis which is critical for self-cleaning effects. If the size of the droplet is appreciable enough to be affected by gravitational effects, then the transition from the Cassie-Baxter state to the Wenzel state is irreversible which destroys the liquid repellent property of the lyophobic fabric. It was also shown that this forced transition (reversible or irreversible) was achieved by evaporation or condensation of drops or by external pressure application i.e. dynamic impacts, sagging of liquid curvature between fibers, hydrostatic pressure, etc. External pressure application was adopted for the robustness experiments. They used two volumes of drops: (1) Large drops which required less pressure application for transition due to the hydrostatic pressure exertion by the drops on the substrate. (2) Small drops which have negligible gravitational influence on them required higher pressures.

Gao and McCarthy[40] have emphasized the proper usage of the terms “hydrophobic” and “hydrophilic”. They state that these terms are relatively qualitative and that advancing and receding contact angles are capable of characterizing wettability of a surface better than the static contact angle. Teflon® that is generally considered hydrophobic was proved to act differently in their experiments. This is closely related to the observations made in this research as anomalies were viewed with liquid behavior to the solid surface of Teflon®.

The aim of producing robust and strong lyophobic surfaces is rampant in much technological research. Most of the Si etched surfaces are non-durable as well as they are subject to

mechanical deformation which in turn would affect the liquid repellent properties. Robustness could be a quantitative evaluation of superoleophobicity besides contact angle and roll-off angle measurements.

Today, developments are aplenty in manufacturing superlyophobic surfaces. Superhydrophobic/ superoleophobic surfaces are achieved by chemical treatment with low surface energy substances containing fluoro compounds or by fabricating extremely rough surfaces.[41,41b,41c] Hayn et al[42] prepared highly lyophobic woven fabric by treating it with perfluoroalkyloxysilane in microwave. Superhydrophobicity was achieved by using water as a catalyst for a smooth coating. Superoleophobicity required roughening the surface with a base catalyst that created multi-scale hierarchy. Ohkubo et al[43] roughened aluminum (Al) substrate by sandblasting and electrolytic etching and treating it with fluorocarbons (chemically adsorbed monolayer). The water and hexadecane contact angles were 158.9° and 139.6°. Tuteja et al[20] designed a robust non-wetting surface with re-entrant structure. Cao et al[44] fabricated a hierarchical micro and nanoscale silicon (Si) film by gold-assisted etching and proved that such overhang structures induced the superhydrophobic and superoleophobic phenomenon. Liu et al[45] used fish scales to mimic a superoleophobic surface based on the water-liquid-solid interface. Fish scales are extremely hydrophlic and oleophilic in air, but exhibit excellent oleophobicity in water with oil contact angles of 156.4 ± 3°. Fish scales were used as templates to make PAM replicas which had volume-swelling properties in water and contact angles as high as 162.6 ± 1.8° were achieved.

Cao et al[44] pointed out the problems in quantitatively evaluating the stability of oil in the Cassie-Baxter state. Im et al[46] tested the robustness of a polydimethylsiloxane (PDMS) trapezoidal surface by immersing it in deionized water and methanol. Extrand[47] pointed out that it was essential to achieve a balance between the pressure of suspending a drop between surface protrusions or asperities and the pressure of retaining the drop on the surface. Maximizing suspension pressure was achieved by changing asperity size and spacing ratio. This also increased retention pressure. In order to strike a balance, the change in surface features was succeeded by chemical manipulations of the surface. This ensured that drops under external pressures did not wet the substrates.

Tuteja et al[49] patented a tunable superoleophobic surface with fluorinated nano particles. It is capable of switching between wetting and dewetting. Development of such extremely liquid-repellent surfaces requires the design of substrates that facilitates the formation of a composite interface with any liquid irrespective of its surface tension. This composite Cassie-Baxter interface is dependent on two criteria with any contacting liquid: (a) high apparent contact angles on patterned surfaces and (b) robustness of the composite interface against external mechanical pressures that causes the scaling of the energy barrier to a wet surface with a lower free energy.

The common testing methods followed by Tuteja et al (2010) for mechanical durability of the fabrics involved stretching the fabric multiple times and mechanically rubbing the fabric surface by hand. Stretching of the fabric changed the pore size within the fabric (leading to a

change in the value of the design parameters H^* and T^* for different liquids. This then allowed for some liquids to wet the fabric and permeate through it, while other liquids remained unable to wet the surface. Generally, liquids with lower surface tensions begin to wet the surface first as the pore size increases. Wetting liquids are able to pass through the fabric. By changing the pore size of the fabric as well as the surface energy of the dip-coating material (as guided by the design parameters H^* and T^*), it was possible to separate various liquids, even though there was a very slight difference in surface tensions. All of these experiments did not damage the coating which was confirmed by imaging the microstructure of the fabric using a scanning electron microscope or reduced performance (as determined by measuring the contact angles with various liquids, before and after testing). No tests were conducted to test the robustness of the designed surfaces.

2.2. Wettability and its mechanics

Wetting is caused by the intermolecular interaction between a liquid and a solid. Wetting is a thermodynamic process involving free energy change that determines the spontaneity of wetting of a surface and the magnitude of external force required to overcome the resistance to wetting. A textile surface is often times wet by a liquid which has a lower surface tension than a higher surface tension liquid like water; in addition the wetness is magnified when the pressure applied on the liquid is sufficient to cause it to penetrate the surface of the woven or knit structure. The amount of wetting is a direct contribution of the surface roughness.[7] The wettability also depends on the magnitude of the adhesive and cohesive forces.

2.2.1. Surface characteristics

Superoleophobicity is a property of the surface chemistry and the physical condition of the solid-liquid interface. The exact surface composition of a surface is an important characteristic to determine wetting. Hence, a surface with high surface energy is more likely to be robust as it resists wetting. The forces of adhesion and cohesion within a droplet define whether spreading of the droplet occurs. An important character for any interface is surface free energy which is the existence of free atoms at the surface. Surface energy is defined as the energy required to create a surface with unit area and it quantifies the disruption of

chemical bonds when a surface is created.[10] If pressure is applied to liquid on rough surface and thereof, removed subsequently, two scenarios arise: (a) the surface free energy recovers the interface by re-creation of its bonds or (b) new wet interfaces are formed due to liquid imbibitions. The former case would be considered as a robust surface, while the latter insignificantly robust. Adhesive forces also adversely affect robustness if there is a high actual contact area between the liquid and the protrusions. Dense fibers favor adhesion and if the space between adjacent fibers is small, then the adhesive force between them is greater than the force required to distort them. This would cause the fibers to stick and this is yet another reason to have adequately spaced protrusions or fibers for stability. Thus, at different surface features, surface tension, droplet size and volume, reaction of the surface to weight, friction, drop pressure, wettability, and protrusion or fiber density affect the robustness factor.

The distance (*2d*) between two adjacent fibers in a woven fabric structure is an important determinant of the extent of robustness of a surface. It is this distance between, along with the density of a liquid and the liquid surface energy that determines the curvature or sagging of the liquid between the adjacent fibers. If the distance is too large, impalement would occurs leading to the establishment of a Wenzel model. If the distance is too small, entrapment of the liquid drop between the surface features would occur; this would cause wetting due to capillary action. In both cases, the fully-wetted Wenzel state would be established eventually. In the latter case, sometimes a reactive force acts to overcome the capillary action and push the droplet back to the surface. This type of a structure is called a re-entrant structure.

2.2.2. Contact angle

The primary parameter that characterizes wetting is contact angle which is defined as the angle formed by a liquid at the point of interaction of a solid-liquid-air interface.[11] Wettability is an inverse measure of contact angle. The tendency of a liquid to spread over the surface increases as the contact angle decreases.[12]

For evaluation of surface tension and wettability, the contact angles are measured (Kovats, 1989).[13] The continuum of relationship between wettability and contact angle can be seen in Table 2.2. Young's Equation predicts the surface tension on the basis of contact angles measured using a goniometer.

Table 2.1. Variation in Wetting for Different Apparent Contact Angles, θ on Smooth Surfaces

Contact Angle	Degree of Wetting
$\theta \leq 5^{o}$	Complete
$0^{o} < \theta < 90^{o}$	High
$90^{o} \leq \theta < 180^{o}$	Low
$\theta \geq 175^{o}$	No

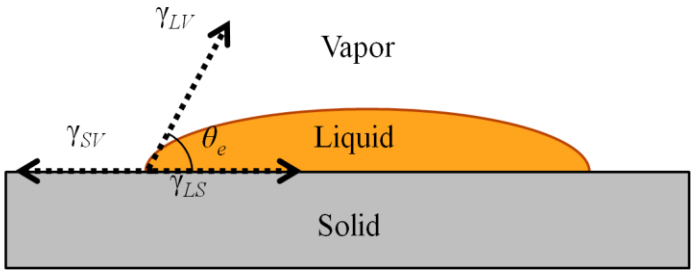

Figure 2.2. A drop on a flat surface acted upon by interfacial energies at the surface.[14]

The curved surface, for example, the cross section of a sphere or a fiber, always provides a point along its length such that there is a relationship between the air, vapor, and solid interfacial energies.

$$cos\theta_e = \frac{\gamma_{SV} - \gamma_{SL}}{\gamma_{LV}} \quad (2.1)$$

where, θ_e is the equilibrium contact angle when the different interfaces are in phase, and γ_{SV}, γ_{SL} and γ_{LV} are the respective interfacial energies. θ_e determines the wettability of a material. Figure 2.1 shows the positions of the different interfaces as well. Young's Equation represents the contact angle as a well-defined property that depends on the surface tension coefficients of solid, liquid and gas.[15]

Flat surfaces and rough surfaces

A smooth surface will have less surface area than its rough counterpart to interact with the liquid. For a unit area of a rough surface, the surface area is greater and hence a proportionally greater increase in the intensity of surface energy as compared to a flat surface of the same area.[7] The material surface determines the wetting behavior of liquids.[16] Very few solid surfaces are ideally smooth, for which Young's contact angle is valid. In most instances, the surface is rough which leads to partial wetting with the liquid drops perched on the upper protrusions of the roughness and the lower part being filled with air.[17] When the surface is roughened, the liquid surface free energy decreases which results in two possible

contact angles, the Wenzel apparent contact angle or the Cassie-Baxter apparent contact angle.[18]

Wenzel and Cassie-Baxter models

Two distinct models, developed by Cassie and Wenzel, are commonly used to explain the effect of roughness on the apparent contact angle of a drop sitting on a surface. The roughness of a surface can be determined by Wenzel and Cassie-Baxter equations. Wenzel is a state where the liquid wets the grooves of the wet surface while the Cassie-Baxter state is when the liquid drop sits on the rough peaks of the porous surface. The former has a high contact angle hysteresis, while the latter has a low contact angle hysteresis which makes the presence of a composite interface evident. With regard to robustness, a drop can be caused to transition to the Wenzel state by applying external pressure. The eventual location of the liquid after the pressure has been removed determines the robust nature of the fabric. If the fabric is dewet by the liquid to the Cassie-Baxter state with a high contact angle, then the surface is considered to be robust enough to maintain its state of superhydrophobicity or superoleophobicity. If the fabric is completely wet, then the surface is not considered to be robust to withstand forces.

A homogeneously wet surface is described by the Wenzel model. The Wenzel model explains how a rough surface is wet. It recognizes that surface roughness increases the available surface area of the solid, which geometrically increases the Wenzel contact angle, θr^W for the surface.

This model is described as,

$$cos\theta_r^W = rcos\theta_e \qquad (2.2)$$

where, r is the ratio of the total area wet by the liquid to the apparent surface area in contact with the liquid, θr^{CB} is the measured or apparent contact angle.[7] For a Wenzel surface, r is always greater than 1. This would lead to two phases based on the Young's contact angle, θ_e:

- If $\theta_e < 90°$, then the already wet surface will become more "philic".
- If $\theta_e > 90°$, the surface will become "phobic".

This roughness factor, r does not completely define the texture as it does not involve the shape of the rough feature. This paved the way for the extension of the Wenzel model to the Cassie-Baxter model.[19]

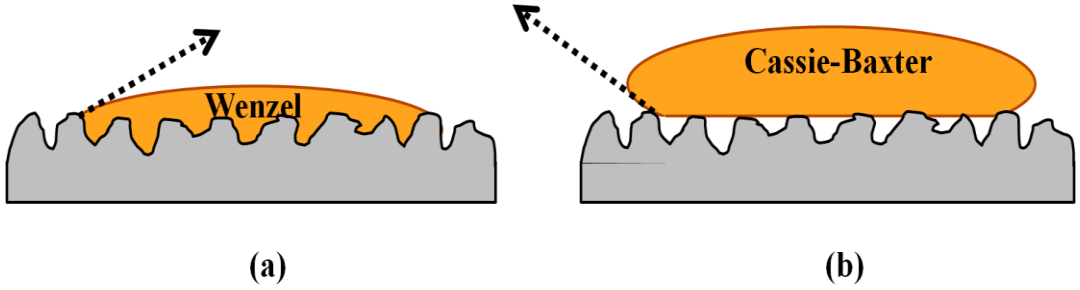

Figure 2.3. Two wetting models of a liquid droplet sitting on a rough surface: (a) Wenzel model and (b) Cassie-Baxter model.[14]

Figure 2.3 shows the completely wet and partially wet phases of a droplet on a rough surface. The Cassie-Baxter model, apparent in the lotus leaf proposes that the superhydrophobic and superoleophobic nature of a rough surface is caused by air remaining trapped below the water droplet. This results in a composite interface with the drop sitting partially on air and the upper features of the rough solid. The robustness of a surface is directly proportional to its Cassie- Baxter state.

The contact angles on such a heterogeneous (two materials) rough composite surface is described as the Cassie-Baxter apparent contact angle, θr^{CB},

$$cos\theta_r^{CB} = f_1 cos\theta_1 + f_2 cos\theta_2 \qquad (2.3)$$

where,

$$f_1 = \frac{\text{Surface area of liquid in contact with material 1}}{\text{Projected area}}$$

$$f_2 = \frac{\text{Surface area of liquid in contact with material 2}}{\text{Projected area}}$$

θ_1 and θ_2 are the respective contact angles[8]. Since textile materials are porous in nature, f_1 is the surface area of the liquid in contact with the solid portion divided by the projected area, and f_2 is the surface area of the liquid in contact with the air pockets in the interstices of the fabric divided by the projected area. Since $\cos\theta_e$ of air is -1, the above mentioned Cassie-

Baxter model transforms to:

$$\cos\theta_r^{CB} = f_1 \cos\theta_e - f_2 \qquad (2.4)$$

When there is no trapped air, the liquid seeps into the interstices and f_2 becomes 0 while f_1 becomes the roughness factor, r in the Wenzel model (Equation 2.1).

Recently, Marmur[9] modified Equation 2.4 to be more adaptive to a porous texture.

$$\cos\theta_r^{CB} = r_f f \cos\theta_e + f - 1 \qquad (2.5)$$

where, r_f is the roughness factor, f is the liquid-air interface occluded by the solid surface. (1 - f) replaces f_2 from the original equation for the flat liquid-air interface (Equation 2.5). Wenzel is a special case of Cassie-Baxter when $r_f = r$ and $f = 1$. The latter is possible only if the surface is homogeneously the same. Marmur says that in order for the liquid to be in its final location with the minimum free energy for the equilibrium state, the above model would be realized if $f = 1$ and $\theta_e = 180°$. Such a contact angle is realized only if the droplet is suspended completely in air or vacuum. This implies that a Wenzel model cannot be "phobic": Cassie- Baxter model will be required to best describe a "phobic" surface.

Meta-stable Cassie-Baxter model

Thermodynamic arguments can be used to determine whether a rough hydrophobic surface will stay in the Wenzel or the Cassie-Baxter state.

The existence of a meta-stable Cassie-Baxter state on surfaces with Young contact angles less than 90° was stated by Marmur.[9] This is an intermediate region during the transition from the non-wetting interface to a fully-wetted one. The local liquid curvature between adjacent fibers is important and this depends on the robustness factor which is also observed. Marmur's proposition of the transitory existence of a composite regime at a local minimum of free energy rather than a global minimum also aids the design of a re-entrant model. This forms the basis for superoleophobicity. Marmur modified the Cassie- Baxter Equation to a form best suited for porous surfaces.

A surface that has a re-entrant portion of the surface (or negative curvature) enhances the contact angle with any liquid.[20] Thus, the re-entrant surface leads to the drop sitting partially on air with high overall contact angles (Cassie-Baxter state). This Cassie-Baxter state is, however, meta-stable as the total energy of the system decreases significantly when the liquid advances and completely wets the surface leading to a homogeneous interface. However, this composite interface configuration is not the true equilibrium state as the fully wetted interface leads to a lower overall free energy. The fully-wetted interface has a lower free energy density as compared to the composite interface and it becomes the thermodynamically favored state. However, it is clear that the correct choice of surface texture can lead to the formation of meta-stable (energetically trapped) composite interfaces, and extremely high contact angles, even though the solid surface by itself may be hydrophilic. It should be mentioned that the lower the value of θ, the more the liquid wets the curved surface, leading

to higher contact angle hysteresis, even with the composite interface. Thus, a surface in the Cassie-Baxter state does not necessarily have low hysteresis, as is widely believed. Surfaces without curvature or having only a protruding surface cannot lead to a composite interface if $\theta_e < 90°$, as the Young's Equation is not satisfied at any point other than for complete wetting.

The contact angle with a low-surface tension solid is greater than that with a high-surface tension one. The contact angle with the surface inside the liquid drop is the same irrespective of the non-uniformity of the surface (i.e. intrinsic contact angles). The liquid comes in contact with the substrate of the rough surface if the Young's contact angle is smaller than a critical contact angle, θ_c. Also, when a smooth surface is progressively roughened, there is a possibility of a reversible transition from Wenzel to Cassie-Baxter state at the transition angle, θ_c,

$$\theta_c = \frac{-(1-f)}{r-f} \tag{2.6}$$

From Equation 2.6, it is apparent that $\theta_c > 90°$, and this would be the stage when Cassie-Baxter state is attained. But this will not be possible in the case of liquids with low surface energies, whose equilibrium contact angle, $\theta_e < 90°$. This can be achieved only by lowering the surface energy of the solid by geometrical or chemical modifications. Figure 2.3 shows the different wetting transition regimes. The strength of the metastability is inversely proportional to the substrate surface tension and the surface energy of the liquid.

The modified Cassie-Baxter Equations cannot be used for further experiments as they were modified to suit a porous protrusion model. A superoleophobic surface can be achieved by placing the Wenzel and Cassie Equations in thermodynamic perspective. A surface satisfying $\frac{d(r_f f)}{df} = -\frac{1}{cos\theta_e}$ and $\frac{d(r_f f)^2}{df} = 0$ is said to be in a meta-stable heterogeneous state with the Gibb's free energy at a local minimum i.e. a rough Cassie-Baxter surface; but if $\frac{d(r_f f)^2}{df} < 0$, then homogeneous wetting is achieved which is at a global minimum of Gibb's free energy. The stable thermodynamic states are attained at global or local minima before the liquid penetrates the texture.[9]

Figure 2.4 shows that for lyophobicity, $\theta_c < \theta_e < 90°$, where θ_e is the contact angle on a flat surface, and θ_c depends on the surface design, the apparent contact angle θ_r^W should be given by the Wenzel model (Equation 1). If θ_e is larger than θ_c, air remains trapped below the drop, which sits on a composite surface made of solid and air. However, it has often been reported that the Cassie regime can also be observed for $\theta_c > \theta_e$, in spite of a higher energy. This meta-stable situation is represented by the dotted line.

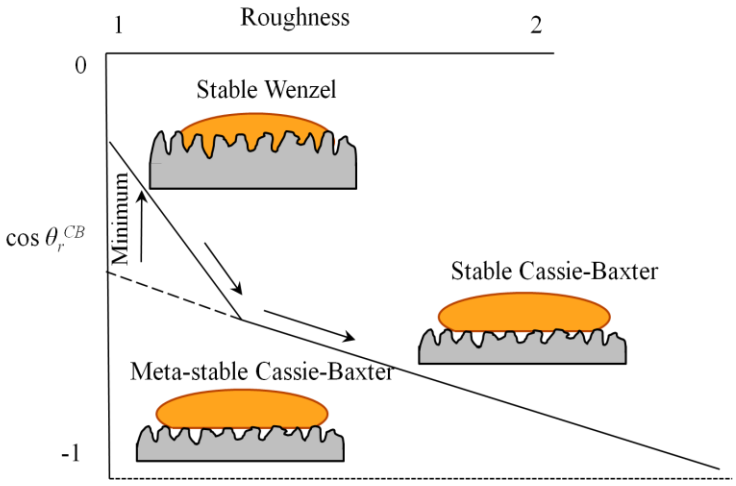

Figure 2.4. Wetting transitions with reference to minimum free energy.[10]

In order to cause the transition from a higher energy Cassie-Baxter state to the lower energy Wenzel state, an energy barrier has to be overcome i.e. work must be done to cause the transition.[21] The work done depends on the surface energy and the surface roughness.

It was observed that for droplets with low surface tension, after the removal of the force, a small amount of liquid is sucked into the texture, and the remaining drop sets on a patchwork of solid and liquid, the vapor phase supporting the drop is replaced partially by liquid. This is similar to the hemi-wicked state described by.[22] The contact angle in such a case is not zero as the fabric is partially wet with the presence of emerged islands. This is the intermediate state pointed out by Patankar[23] wherein, although Wenzel state would have the lowest energy, the liquid fills the grooves of the rough surface and the lower curvature rests below the contact line of the Cassie-Baxter state without completely filling the valleys of the pores.

2.2.3. Contact angle hysteresis

A drop in motion on a tilted surface will exhibit greater contact angle in front (advancing contact angle) than at the back of the droplet (receding contact angle) due to roughness and this difference is the contact angle hysteresis. Surfaces with low hysteresis will have low liquid roll-off angles which depend on the surface tension of the solid, its topography, and size of the droplet.[11a, 19] Although apparent contact angles on any surface are governed by fraction of solid in contact with a liquid, the amount of contact angle hysteresis can vary significantly depending on the details of each individual surface texture. Hence a surface that supports a robust composite interface can also be tailored to enhance or reduce contact angle hysteresis. Low hysteresis results in very small roll off angles, corresponding to easy movement of the liquid droplets on the surface. On the other hand, high hysteresis implies that a significant amount of energy needs to be expended in moving the liquid droplet.[24] This, in turn can be used to adhere the liquid droplet at a particular spot on the surface. Increasing the solid fraction of the surface texture can increase the receding contact angles, while decreasing the solid fraction in contact with the liquid can decrease the robustness. Contact angle hysteresis is inversely proportional to the composite Cassie-Baxter state.

2.2.4. Energy barrier

For a liquid drop on a rough surface, there are two local minima in the free energy corresponding to the composite and fully-wetted regime. The interface which has the lower free energy density becomes the thermodynamically preferred state. If the composite state is

the favored state, then the liquid can be caused to transition to the fully-wet state by providing enough activation energy to force it into the surface texture. Activation energy is the minimum energy that has to be overcome for work to be done. It can be considered as the height of an energy barrier that separates two minima in potential energy. Figure 2.5 shows the height of the energy barrier. When a drop of liquid is deposited on a rough surface, the drop would try to occupy the location with the lowest minimum in free energy. The surface groups would re-orient themselves to accommodate this occupation of the minimum free energy state.

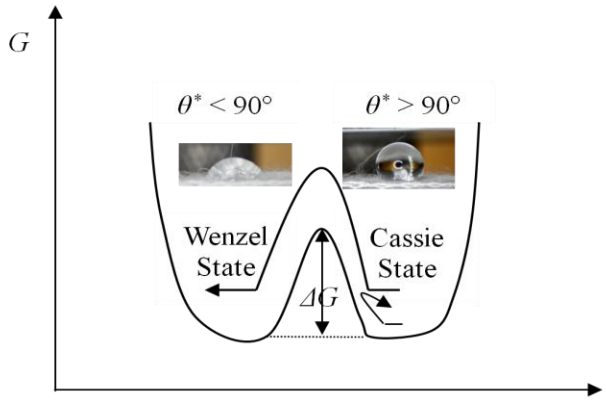

Figure 2.5. Minimization of free energy barrier.[25]

The activation energy can be provided by dropping the liquid drop from a height or external pressure. In the case of the robustometer, the activation energy provided by the force applied on the drop by the Teflon®-coated aluminum plate works in two ways:

1. To cause the drop to move from one fiber to the other while spreading. Here, the activation energy is the height of the energy barrier that separates the energies of movement between two adjacent fibers:
2. To cause the transition from the Cassie to the Wenzel state during imbibitions. The lower the adhesion of the drop to the substrate, the higher is the energy barrier to cause the Wenzel transition.

As the force is applied on the drop, the sessile drop is squeezed over the fabric such that it starts advancing and it exhibits an advancing contact angle. Alternatively, when the force is removed, the drop starts receding on the fabric and the contact angle decreases to a minimum receding value before the contact retreats. The drop is pulled apart till there is cohesive failure in the middle where it is stretched. The amount of liquid remaining on the fabric depends on the adhesive forces between the drop and the fabric and between the drop and the Teflon® coating. The greater the force of adhesion between the drop and the fabric in comparison to that between the latter and Teflon®, the more the liquid is retained on the fabric with a small residue on the Teflon® and vice-versa.

2.3. Thermodynamic analysis of the wetting state

Thermodynamically, the Wenzel and Cassie-Baxter states are considered to have the local and global minimum in free energy depending on the height of the energy potential separating them. The global minimum is the energetically favored position. From the mode of droplet formation, the liquid can stay in a meta-stable position which is in the local

minimum state.[20, 48, 51] While measuring robustness by the test employed in the present work, if the drop wets the fabric, then the force and pressure taken to transcend from the meta-stable position to the Wenzel state is accounted for; whereas if the drop finds its original location after the release of the external force, then the composite Cassie-Baxter regime is considered to be the stable global minimum in free energy as opposed to the complete wetting phase.

When a liquid drop spreads over the surface, there will be constant changes after the displacement of the initial drop interface. The changes continue until the drop attains minimum free energy when the radius of the drop stops changing. If the total energy of the system rapidly changes with the advancing liquid-solid interface, the fully-wet regime will be attained; if the drop attains the minimum free energy before it starts penetrating to the substrate, the composite partially-wet regime is obtained.[46] Im et al[46] also used the droplet impinging test to test for robustness of their superhydrophobic structure. This test involves dropping the liquid from a certain height. Other methods of applying external disturbance involve electric potentials.[52] To confirm the robustness of superhydrophobic surfaces, researchers made a transition of the wetting state from Cassie-Baxter to Wenzel by pushing droplets [34, 53], or by dropping droplets from a certain height. In particular, He, et al[41a] analyzed the robustness of the superhydrophobicity of micropillared surfaces by comparing two droplet contact angles after droplets were gently deposited and deposited from a certain height.

Vagharchakian et al[54], in their push-and-pull adhesive experiments pointed out that when a surface in contact with a liquid reservoir is retracted, the contact line is pinned to the surface and retracts only when it reaches the receding contact angle, while pushing on the liquid, the contact line starts moving only when the advancing contact angle has been attained. This trend is observed in the robustness experiments as well.

2.4. Robust parameters

Tuteja et al[48] have demonstrated the possibility of engineering a textured re-entrant surface that repels a range of liquids by suitably designing geometrical parameters and altering the surface energy of solids by electrospinning and dip-coating processes. Achieving appropriate design features by manipulating the surface chemically and increasing the equilibrium contact angle. This helps display high contact angles and supports a robust solid-liquid-vapor interface that is stable under maximum breakthrough pressure. This study can be applied only to scales of hierarchical roughness. They introduced the use of a third parameter i.e. robustness besides surface modifications and topographical modifications to create robust superoleophobic surfaces. Re-entrant structures were designed for super-nonwetting fabrics that are resistant to a wide range of liquids such as water, hydrocarbons, and toxic chemicals .Re-entrant structures are those that are capable of pushing liquid under pressure back to surface from within the texture after pressure removal. However, the presence of re-entrant texture is not a sufficient condition for producing robust superhydrophobic or

superoleophobic surfaces. This is due to insufficient activation energy required to make the irreversible transition from a composite interface to a fully wetted interface. Further, even though a Gibbs free energy approach can reliably predict the existence of a composite interface, its ability to estimate the robustness of the regime is limited as the analysis typically assumes a locally flat liquid-vapor interface[9, 20] i.e. it does not take into account the sagging of liquids between fiber spaces. With actual droplets, possessing significant internal Laplace pressure or under externally applied pressure, considerable sagging of the liquid-vapor interface can occur and the actual failure of the composite regime typically originates not from the activation energy required to transition between the composite and fully-wetted states, but from the sagging of the liquid-vapor interface. Hence the robustness of a composite interface can be significantly lower than the values obtained using Gibbs free energy calculations[49].

In order o provide a relative measure of the pressure required to cause the breakdown of a composite interface, Tuteja et al[20] developed four dimensionless parameters: D^*, the spacing ratio, T^*, the robustness angle, H^*, the robustness height, and A^*, the robustness factor which determines the tendency to resist sagging or wetting. D^* is the spacing ratio of the surface texture which is related to the apparent contact angle, θ_r^{CB}. It is dependent on the distance between fibers, d, and the radius, R of the fibers. The value of d or R i.e. surface feature determines the non-wetting state. The change in the radius or distance between fibers will affect the design parameters.

An increase in D^* is a direct implication of less solid fraction in the texture, which consequently effects a higher apparent contact angle.

$$D^* = \frac{d+R}{R} \tag{2.7}$$

H^* relates to the sagging of the liquid-vapor interface as a result of pressure (Laplace pressure, external pressure or gravity). H^* compares the maximum fabric interstitial depth with the sagging depth of the interface and determines the robustness pressure that causes the liquid-vapor interface to be distorted enough to trigger sagging of liquid into the fabric structure. H^* compares the breakthrough pressure (P_H) to cause the liquid sag to the maximum pore depth, with a reference pressure for millimeter drops. The reference pressure

is the closest to the minimum pressure difference across the liquid-solid-vapor interface. Complete wetting will eventually occur when $H^* >> 1$ because the meta-stable state is only at a local minimum of free energy and it will always occupy a lower free energy level eventually.

$$H^* = \frac{2(1-\cos\theta_e)R\gamma_{LV}}{d^2} \tag{2.8}$$

The breakthrough pressure was based on the balance of forces between the pressure within the liquid to the surface tension forces.

$$\mathrm{P}\cdot(\text{interfacial area}) = \gamma_{LV}\cdot(\text{contact line length})\cdot\sin\delta\theta \tag{2.9}$$

If length, l of the fibers were considered, Equation 2.9 becomes,

$$P_H 2d \cdot l = \gamma_{LV} 2l \sin \delta\theta \tag{2.10}$$

$$P_H = \frac{\gamma_{LV} \sin \delta\theta}{d}$$

$$P_H = \frac{2R(1-\cos\theta_e)\gamma_{LV}}{d^2} \tag{2.11}$$

Equation 2.11 was used to quantify the breakthrough pressure required to break the meta-stable condition and establish the priori existence of a non-wetting interface.

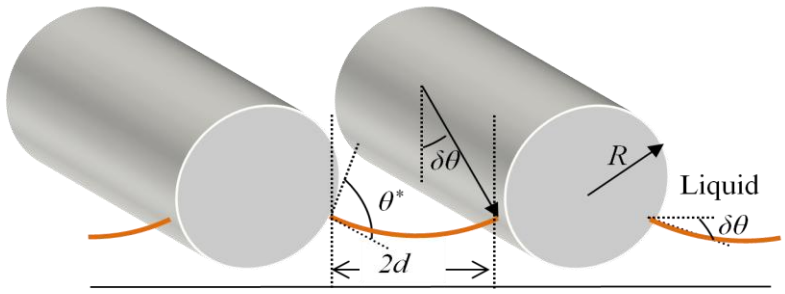

Figure 2.6. Schematic of the sagging of the liquid-vapor interface on application of pressure.

Meta-stable state does not exist for every protrusion feature due to other forces acting on the sagging liquid's curvature. These forces would easily destroy the meta-stable state, especially when the energy barrier between the liquid drop's local minimum free energy and the equilibrium state is very small. T^* depends on the sagging angle, $\delta\theta$ (= θ_r^{CB} - Ψ_{min}). For a robust surface, the geometric angle, Ψ of the protrusion has to be greater than θ_e and less than

90º. Complete wetting would occur at $\Psi = 0°$ for a simple woven structure with cylindrical monofilaments when sagging height or sagging angle of the curvature increases (Figure 2.6). Thus, a rough structure possessing a high interstitial depth will have an extremely high value of H^*. However, even if the composite interface on a surface is expected to be extremely resistant to failure with its large interstitial depth, it can still readily fail due to a shift in the local contact angle as a result of the sagging liquid-vapor interface. Initially, on any rough surface, the liquid-vapor interface makes an angle with the solid substrate. As the applied pressure increases, the liquid-vapor interface becomes more and more severely curved or distorted. This leads to a decrease in the contact angle between the liquid and the solid, until

eventually it becomes equal to the equilibrium contact angle, θ_e for the liquid. Any additional pressure will make the interface move and penetrate into the solid structure. Thus, the composite interface transitions to the fully-wetted interface when the sagging angle $\delta\theta = \theta_e - \Psi_{min}$ (thus any liquid with $\theta_e < \Psi_{min}$ will fail immediately). The robustness of any composite interface will be proportional to the minimum between the values of the two robustness parameters, H^* and T^*.

$$T^* = \frac{l_{cap}\sin(\theta - \psi_{min})}{2d} \tag{2.12}$$

To achieve both extremely high apparent contact angles and a robust composite interface, the design parameters D^*, H^* and T^* ought to be at a minimum. Increasing the spacing between the fibers, d leads to higher D^* values, however, this also leads to lower values of both T^*

and H^* corresponding to severe sagging of the liquid-air interface. This, in turn, allows for easier liquid penetration through the structure. Therefore, there has to be a trade-off between robustness and surface texture. A low θ_e with high D^* will lead to a meta-stable state. Increasing the surface chemistry (θ_e) will reduce the surface roughness (D^*) thereby increasing the robustness of the fabric and making it less vulnerable to penetration. According to Chhatre et al[50] for all surfaces, the criterion for robustness is considered to be $A^* >> 1$. Complete wetting occurs when the liquid sags to the extent of the height at values of $A^* \leq 1$.

$$\frac{1}{A^*} = \frac{1}{H^*} + \frac{1}{T^*} \tag{2.13}$$

These design parameters theoretically help determine the breakthrough pressure which would lead to the afore-mentioned increases, thereby assisting in modeling a robust surface topography.[48]

For this research, these design parameters are used to compare the measured robustness values with the maximum predicted values to determine the wetting behavior at different pressure. This gives an understanding of the behavior in which the liquid follows the surface texture and the transitions caused by it. At present, there is no viable method to quantitatively measure the robust breakthrough pressure.

Chapter 3 Experimental

The experimental section describes the stepwise procedure in carrying out robustness tests for fabrics treated with superhydrophobic and superoleophobic finishes. Initially, three different fabrics were used to characterize the experiment and arrive at pressure parameters and curves. This was followed by using a simple fabric structure to describe the process with reference to the characterization of the instrument used.

3.1. Materials

The liquids that were commonly used for this test were water (surface tension: 72.8 mN/cm), Kaydol (31 mN/cm), and dodecane (25 mN/cm). Although we use low surface energy liquids which are comparable to toxic agents with surface tensions in the order of 24.65 mN/cm (mN/m) to 32.11 mN/cm (mN/m), they might not behave the same way in practice because some liquids might have similar surface tensions, but different molecular packing. For example, a branched chain will not be as regularly packed as a straight chain. This will inadvertently lead to differences in non-wetting behavior (Sharfrin & Zisman, 1960). (Heptadecafluoro-1,1,2,2-tetrahydrodecyl)trimethoxysilane (Fluorosilane, $C_{13}H_{13}F_{17}O_3Si$, Gelest, Morrisville, PA, USA), ammonium hydroxide (NH_4OH, Mallinckrodt Chemical, Raleigh, NC, USA), methanol (CH_3OH, Aldrich), and isopropyl alcohol (C_3H_7OH, Fisher) were used without further purification. Distilled water, Kaydol, and dodecane ($C_{12}H_{26}$, Aldrich) were used as liquids to measure contact angles.

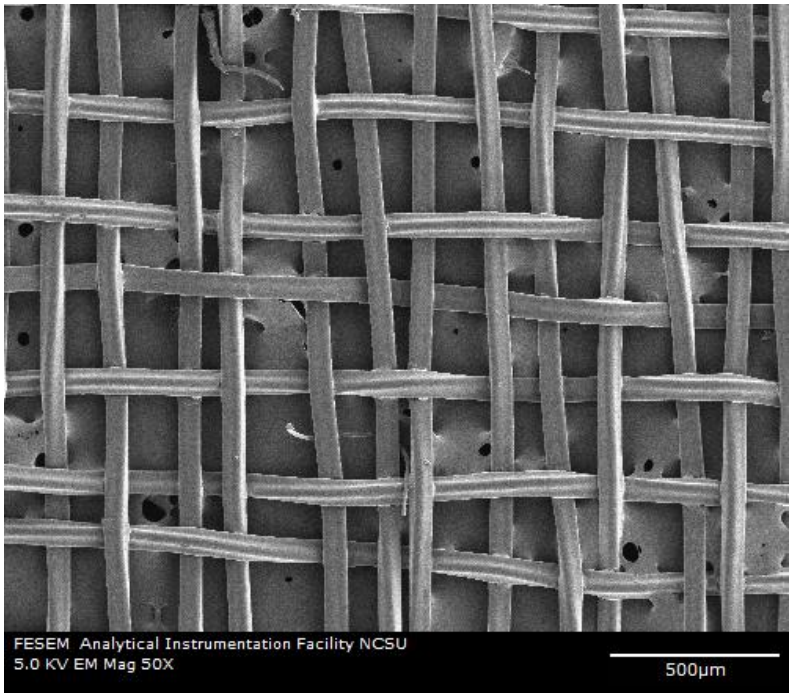

Figure 3.1. SEM of a woven monofilament nylon fabric.

The fabrics that were tested for robustness were the following:

- Flame-retardant (FR) knit: This has anti-microbial and oil/water repellent finishes.
- Flame-retardant woven: This has been treated with oil/water repellent finishes.
- Cotton woven: This has been treated with oil/water repellent finishes.

For detailed analysis, monofilament woven nylon fabric with a thickness 0.18 mm and base weight of 33.05 grams per square meter (gsm) was chemically modified with the superhydrophobic and superoleophobic fluorosilane treatment. The radius of the fibers in the

fabric was measured to be 70.3 µm and the distance, *2d* between two adjacent fibers was 130.3 µm. Figure 3.1 shows the microscopic structure of the woven sample.

3.2. Preparation of rough fabric surfaces

The oil/water repellent treatments are primarily 3 methods i.e. (a) grafting of PFAC8 on nylon 6.6 films and hydro-entangled nylon non- woven fabric, (b) grafting of F-Silane using microwave reaction, and (c) grafting F-silane through wet processing. The fluorosilane application in every method, along with the underlying fiber-to-fiber spacing, leads to the lyophobicity.

4 g/l solution of polyacrylic acid (PAA) ($(C_3H_4O_2)_n$, Aldrich) was prepared with continuous stirring. The fabrics, 10×10cm were padded at 100% wet pick-up and cured at 150^0C for 5 minutes to graft the chemicals. The PAA grafted fabric was then immersed in 4 g/l solution of ethylene diamine (EDA) ($C_2H_4(NH_2)_2$, Aldrich) for 12 hours with continuous shaking. After 24 hours, 1 g 4-(4, 6-Dimethoxy-1, 3, 5-triazin-2-yl)-4-methylmorpholinium chloride (DMTMM, Aldrich) in 10 ml of methanol (CH_3OH, Aldrich) was added to the mixture and the reaction was allowed to proceed for 2 hr. The fabric was washed with distilled water for 2 minutes. Figure 3.2 shows the grafting of PAA on the nylon fabric to increase its reactivity with fluorosilane.

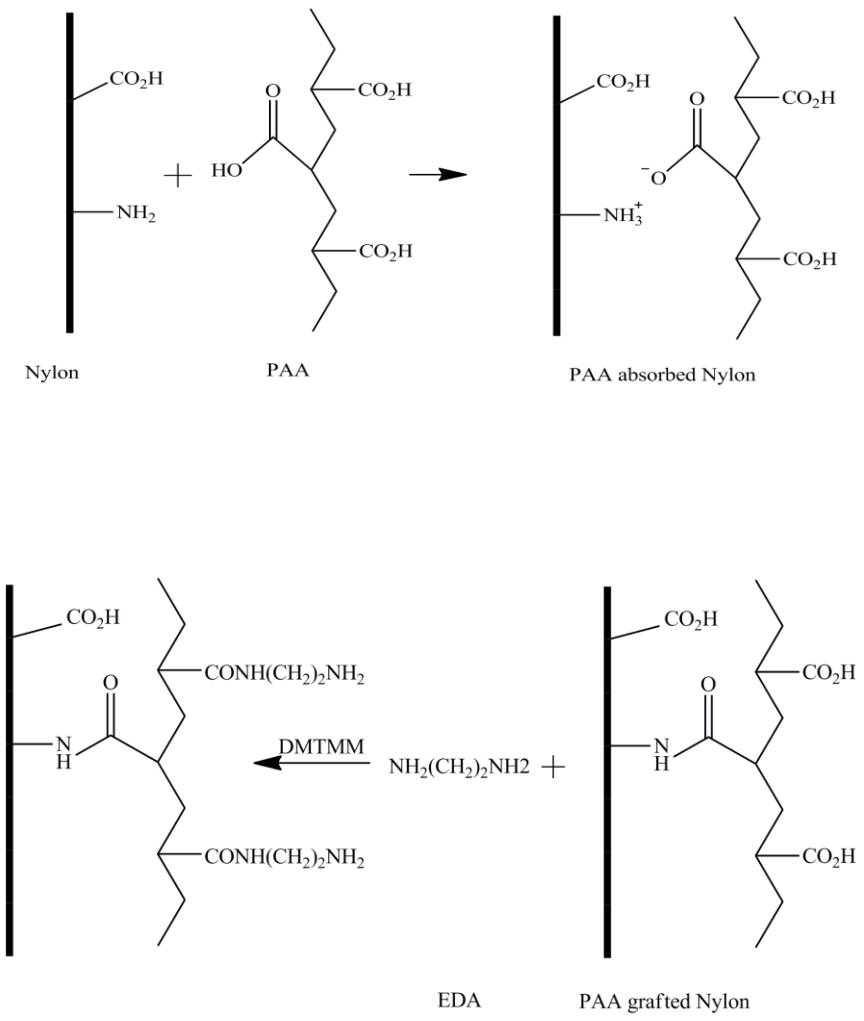

Figure 3.2. Grafting of EDA on PAA-grafted Nylon.[19]

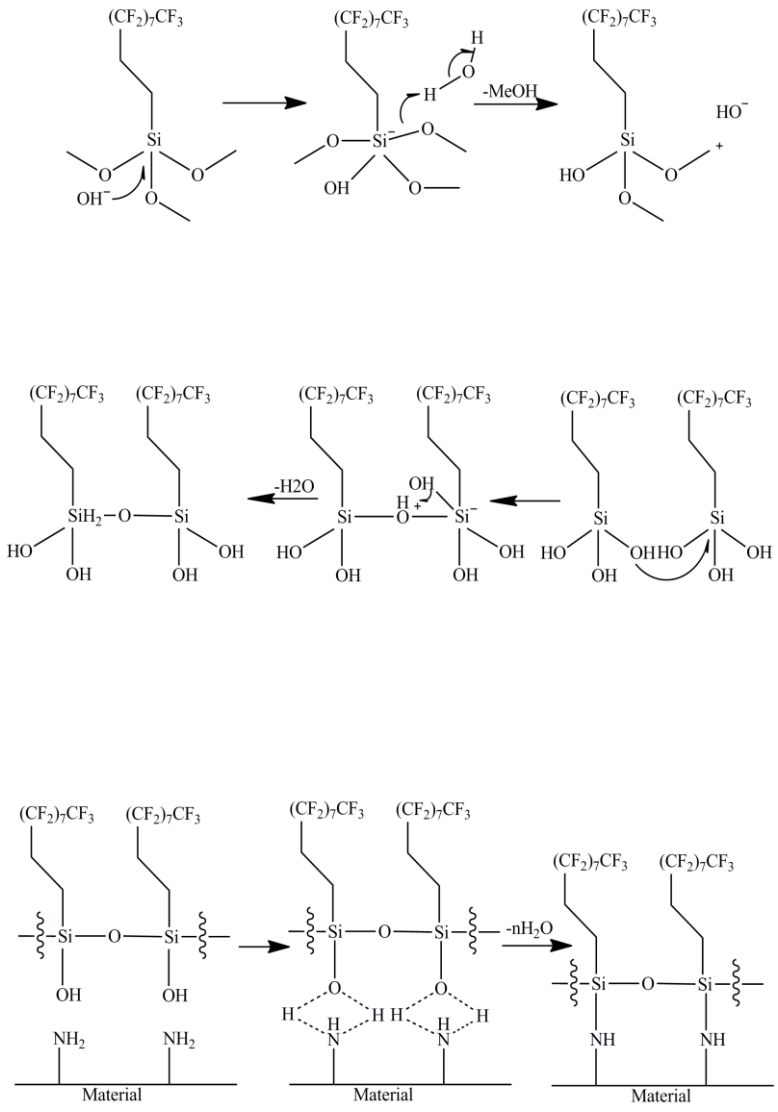

Figure 3.3. Reaction of nylon with a perfluroralkyltrimethoxysilane in alkaline solution.[42]

Figure 3.3 shows the treatment of the PAA grafted nylon with a fluorochemical. In order to provide micro and nano scale protuberances made of fluorosilane on the fabric surface, the fabric was immersed in a solution of 10% fluorosilane in isopropyl alcohol and catalyst and

allowed to partially condense the fluorosilane prior to treating the fabric. The fabric (10 × 10 cm^2) was immersed in the prepared solution, padded to remove excess liquid, and cured in a Mathis unit, which is a laboratory coater & drying unit (maximum sample size 33 × 43 cm, temperature range 20° - 250° C). The fluorosilane-grafted fabric was rinsed with methanol and dried at 100ºC for 2 minutes.

3.3. Robustometer

An aluminum plate whose bottom surface is coated with a Teflon® film is suspended from the density hook on the bottom of a Mettler analytical balance. The fabric is placed on a movable stage which is moved vertically with the electronic control box. Figure 3.4 shows the technical description of the robustometer developed for the robustness tests. To provide a direct measure of the robustness of a composite surface, the robustometer was developed. The robustometer is a modification of the single filament frictometer made by Rame-Hart, Inc.[55] The instrument consists of a moving stage or platform that forms the core of the assembly. This metallic platform moves vertically in a 5mm track with control swtiched on either ends to prevent it from overshooting. The rate at which the stage can be operated can be controlled and varied at various acceleartions via a Compumotor® drive. Speeds of 90 rpm or 5.98 μm/s was used in all tests.

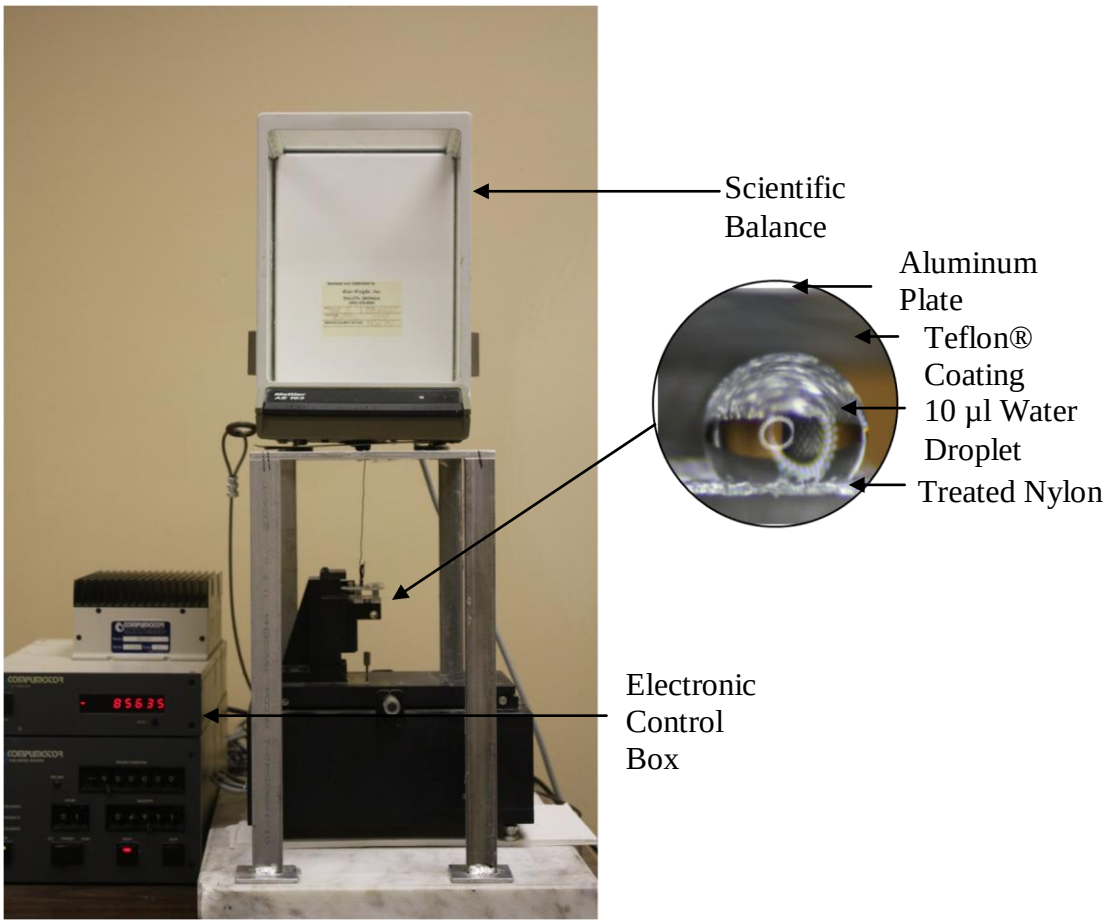

Figure 3.4. Lab-designed robustometer.

The fabrics were conditioned to 65% relative humidity and 21°C and tested under these conditions. The fabric is mounted on the platform with a U-shaped front opening in such a way that when the liquid drop is placed on the fabric, it rests on the fabric above the U, so there is nothing but air under that protion of the fabric. The test weight that is applied on the drop when the stage is moved upwards is a light Teflon®-coated aluminum plate that is suspended by a thin aluminum hook from the support hook of a Mettler® AE 163 analytical

balance. The force applied is observed on the balance in gram units. The motion of the platform is controlled by an on/ off swtich on the electronic box that controls the motor. The box also has controls to move the platform upward or downward. Velocity and acceleration can be preset.

The robustness test was carried out by placing a 10µl water droplet on a 15 mm × 15 mm fluorosilane treated sample, which was mounted onto the moving platform of the robustometer. A plate coated with Teflon® was suspended from a weighing balance, exactly above the drop (Figure 3.5 [a]). The platform was then moved up by a motor unit, towards the plate at a constant rate (Figure 3.5 [b]). The drop is constantly monitored. The applied weight and displacement (in motor units) are observed to plot the curve. Once the applied weight reaches a constant, it is indicative of the plate being lifted off its support hook on the analytical balance. This causes the experiment to be reversed i.e. the fabric platform is reversed in direction (Figure 3.5 [c]). This is the second phase or the force removal phase. The same observations of the weight, displacement, and deformation of the drop are monitored closely.

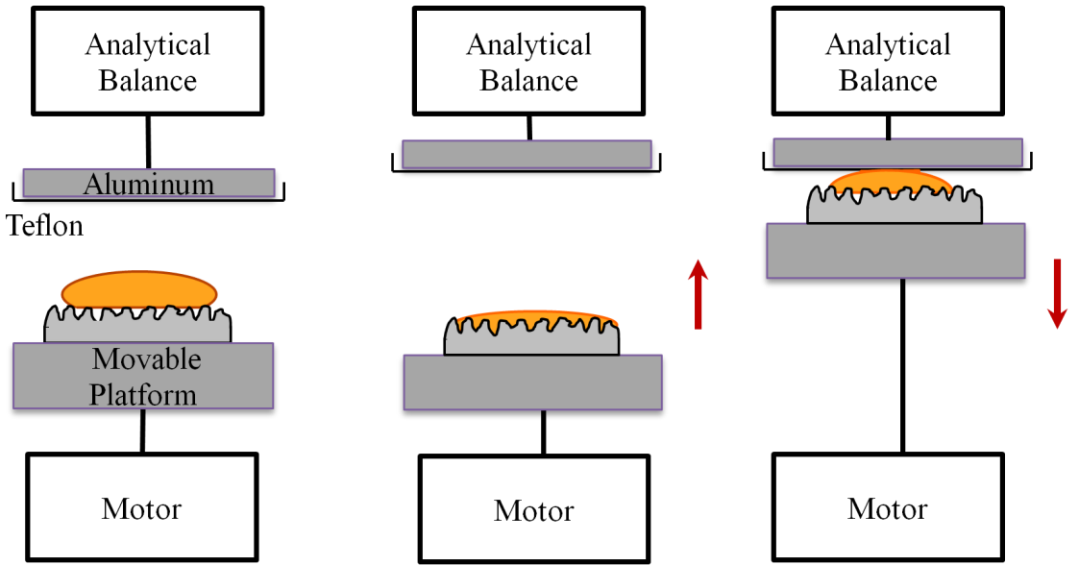

Figure 3.5. Schematic of the working model of the robustometer: (a) Initial Position, (b) Force Application (upward motion of platform with fabric) and (c) Force Removal (downward motion of platform with fabric).

3.4. Characteristics

3.4.1. Scanning electron microscope

The nylon nonwoven fabric was examined using a scanning electron microscope (SEM, Hitachi S-3200N) operated at 5 and 10 kV and magnifications from ×50 to ×50,000. Revolution™ v1.60b24 (4pi Analysis Inc.) was used for image analysis of SEM images. On a rough surface, fiber diameters and the distances between adjacent fibers were measured using this program. Each sample was observed at 5 or more random surface locations.

3.4.2. Contact angle measurements

The contact angles of water, Kaydol and dodecane on the prepared surfaces was measured from sessile water drops using a lab-designed goniometer at 20°C. The volume of the drops captured was 10 µl. Mean values were calculated from at least three individual measurements, each on a new spot. The contact angle images were obtained using a high resolution digital camera (Cannon EOS EF-S-18-55IS) attached to a stereo microscope (Meiji Techno EMZ-13TR).

3.4.4. Image development

Image editing was done using Picasa 3 software.The original image was inverted after improving contrast. It was cropped to focus attention on the drop between the Teflon®-coated aluminum plate and the fabric. The original image was slightly tilted so it was straightened for better clarity. All the images in this work were edited in the afore-mentioned manner.

Chapter 4 Results and Discussions

In order to characterize fabrics based on the robustness of their superhydrophobicity and superoleophobicity, a quantitative analysis of the pressure causing wetting by liquids with different surface tensions was developed. This relies on the penetration of a liquid drop and the ability of the fabric texture to push it back to the surface. The shape of the drop and kinetics of wetting of different fabrics by liquids of different viscosities was qualitatively analyzed. The liquids that were commonly used for this test were water (surface tension: 72.8 mN/cm), Kaydol (31 mN/cm), and dodecane (25 mN/cm).

4.1. Topological analysis of fabric

Prior to robustness testing, a simple monofilament woven fabric has to be roughened to make the surface superhydrophobic and superoleophobic. This fabric, before treatment exhibits a Wenzel surface, as it is a porous substrate that gets filled by the liquid. It is necessary to define the Wenzel roughness which has to be greater than a certain number depending on θ_e, for example, $r > 2.5$ when $\theta_e = 110°$ and hence a hydrophobic surface is achieved; for $\theta_e < 90°$, the surface becomes more hydrophilic. Thus, Wenzel roughness is essential to characterize the fabric and observe the change in apparent contact angle and the degree of wetting after the chemical surface modification.

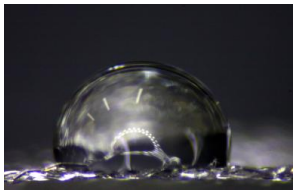

Figure 4.1. Water drop on untreated woven fabric with θ_r^W = 101.2°.

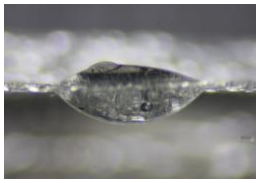

Figure 4.2. Kaydol drop on untreated woven fabric with θ_r^W = 29°.

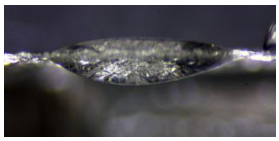

Figure 4.3. Dodecane drop on untreated woven fabric with θ_r^W = 18.2°.

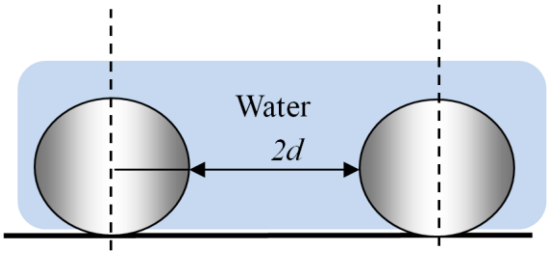

Figure 4.4. Homogeneously wet regime.

$$r = \frac{\pi R + d + R}{d + R} \tag{4.1}$$

Figure 4.4 shows the cross-sectional view of a monofilament woven fabric with a fiber radius, R = 68.2 µm, and average distance between adjacent fibers, $2d$ = 130.3 µm. The Wenzel roughness for this surface with a smooth water contact angle of 72° ($\theta_e^{\ nylon}$ *(water)* = 72°), r is equal to 2.6. The apparent water contact angle according to the model (Equation 4.1) will be, θ_r^W = 36.5°, indicating a highly hydrophilic surface. For such a Wenzel surface, r is always greater than 1, the surface becomes more hydrophobic if the $\theta_e >$ 90° and more hydrophilic if $\theta_e <$ 90° [19] as is evident from the complete wetting with Kaydol (θ_e = 17and dodecane ($\theta_e <$ 5°)in Figures 4.2 and 4.3, respectively.

Textile materials are similar to the lotus leaf and Equation 4.4 can be used to design a proper lyophobic geometrical feature. Prior to designing composite surfaces, surfaces are made "phobic" by roughening and then, apparent contact angles are defined. Figure 4.11 is the similar to the one describing the Wenzel model, but in a different wetting regime. It shows the rough surface of the nylon woven fabric in the cross-sectional view (machine or cross-machine direction). The water wets the upper part of the fibers, but does not reach the substrate. This surface has the potential to be a hydrophobic surface.

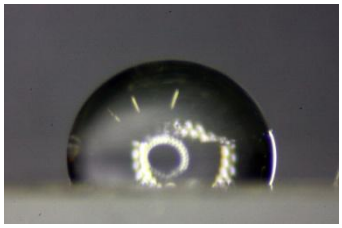

Figure 4.5. Water drop on FS treated nylon film with θ_e = 114.4°.

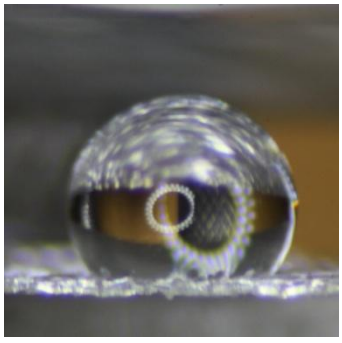

Figure 4.6. Water drop on FS treated woven fabric with θ_r^{CB} = 120°.

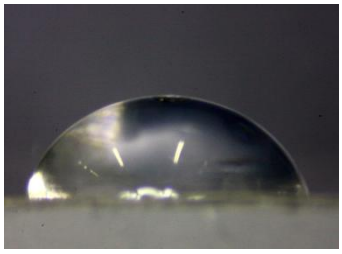

Figure 4.7. Kaydol drop on FS treated woven fabric with θ_e = 67°.

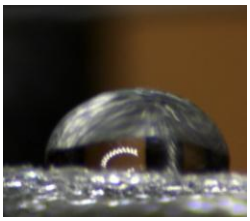

Figure 4.8. Kaydol drop on FS treated woven fabric with θ_r^{CB} = 90.1°.

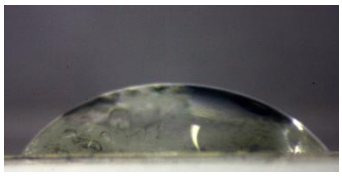

Figure 4.9. Dodecane drop on FS treated woven fabric with θ_e = 48.5°.

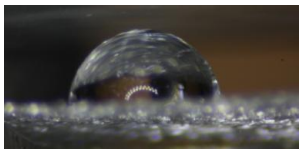

Figure 4.10. Dodecane drop on FS treated woven fabric with θ_r^{CB} = 81.3.

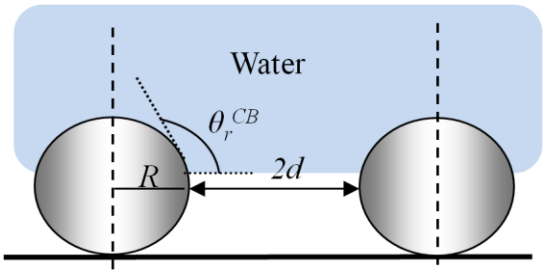

Figure 4.11. Composite regime.

Figure 4.11 shows the cross-sectional view of a monofilament woven fabric with a fiber radius, R = 68.2 µm, and average distance between adjacent fibers, $2d$ = 130.3 µm The Young's water contact angle on a smooth PAA-grafted-nylon film treated with fluorosilane is 107.2°. Based on this, the apparent water contact angle of the composite interface was found to be θ_{CB}^{*} = 135°, indicating a highly hydrophobic surface.

$$r_f = \frac{R(\pi - \theta_e)}{R\sin\theta_e} \tag{4.2}$$

$$f = \frac{2R\sin\theta_e}{2(R+d)} \tag{4.3}$$

$$f = \frac{2\times 68.2\times \sin 107.2}{2(68.2+65.15)} = 0.48$$

Substituting f and r_f in Equation (2.5) results in:

$$\cos\theta_r^{CB} = \frac{R(\pi-\theta_e)}{R+d}\cos\theta_e + \frac{R\sin\theta_e}{R+d} - 1 \tag{4.4}$$

$$\cos\theta_r^{CB} = 1.32\times 0.48\cos(107.2) + 0.48 - 1 = -0.7$$

According to Equation 4.4, an apparent contact angle increases with increasing d for $\theta_e > 90°$. According to Lee[19], when a low-surface tension treatment is grafted on a conventional nylon fabric, superhydrophobicity is achieved as the Wenzel roughness.

Table 4.1. Comparison of Predicted and Measured Contact Angles

10 µl Liquid Droplets	Young's Contact Angle (°) on FS-Treated Nylon Film	Cassie-Baxter's Contact Angle (°)	
		Predicted	**Measured**
Water	107.2	135	120
Kaydol	69	100.5	96.5
Dodecane	48.5	81.4	76.4

Note: The contact angles measured are based on a repeat of 3 or more trials with a deviation of ± 2°.

Table 4.1 shows the equilibrium contact angles of a fluorosilane treated nylon film for water, Kaydol, and dodecane (also seen in Figures 4.5, 4.7, and 4.9). The Cassie-Baxter contact angles are calculated from Equations 4.2, 4.3, and 4.5. These agree well with the measured values recorded in Figures 4.6, 4.8, and 4.10.

4.2. Working model of robustometer

For greater understanding, simple plain woven fabrics were under scrutiny. The fabric was treated with the superhydrophobic and superoleophobic chemical finish. The reason for the detailed analysis of the monofilament woven fabric is due to its continuous geometry. It has long cylinders in the machine and cross-machine direction. Woven structures can be

followed up with the analysis of multifilament fabrics. Multifilaments are more complicated due to the robustness between the yarns and the robustness within the yarns.

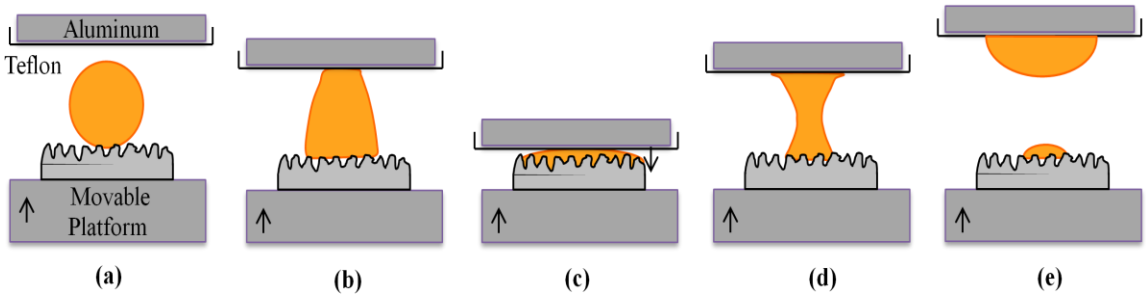

Figure 4.12. The change in droplet curvature at every phase of force compression and relaxation is shown.

Figure 4.12 shows the different modes of compression and relaxation of the liquid drop between the surfaces. As the fabric is raised, the drop rises with it and comes into contact with the upper Teflon® coated aluminum plate (Figure 4.12 [b]); the apparent weight of the contacting plate increases i.e. the force on the plate increases as the liquid offers resistance to the pressure by spreading along the fabric surface. As the fabric is raised further, the circular contact area between the drop and the plate increases, pulling the plate down further and the weight starts decreasing (Figure 4.12 [c]) with the force on the drop increasing. As the platform with the fabric is lowered (bottom), the weight acting on it increases while the force decreases due to the droplet spreading across the fabric surface which supported it (Figure 4.12 [d]).

4.2.1. Phase I: Force application

It was observed that at first contact of the droplet with the upper Teflon® plate, the contact angle was higher due to the air-pockets which correspond to the Cassie-Baxter state. Then, as the pressure acting on the drop increased, the contact angle decreased which could be interpreted as progressive sinking-in of the drop into the fabric texture or spreading across the surface.

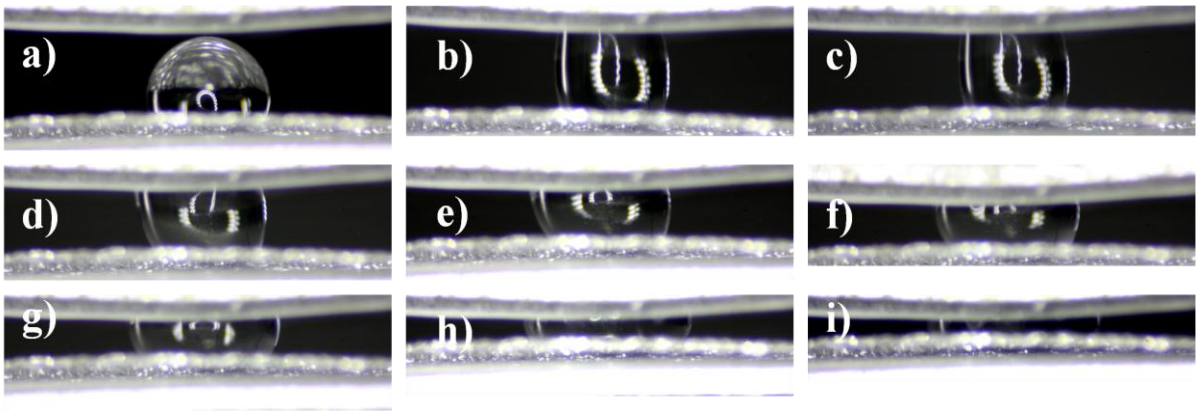

Figure 4.13. First phase of robust pressure testing with force application. The drop is seen to be progressively squeezed as the distance between the upper Teflon® plate and the lower fabric reduces.

Figure 4.13 shows selected images captured by a high resolution digital camera.. The images are those of the 10 µl droplet of water supported on the perfluorinated surface with contact angle of 120° ± 3° being raised up to a Teflon®-coated aluminum plate. The velocity is very small in the range of 90 revolutions per minute or 5.98 µm/s. The following behavior is noticed initially.

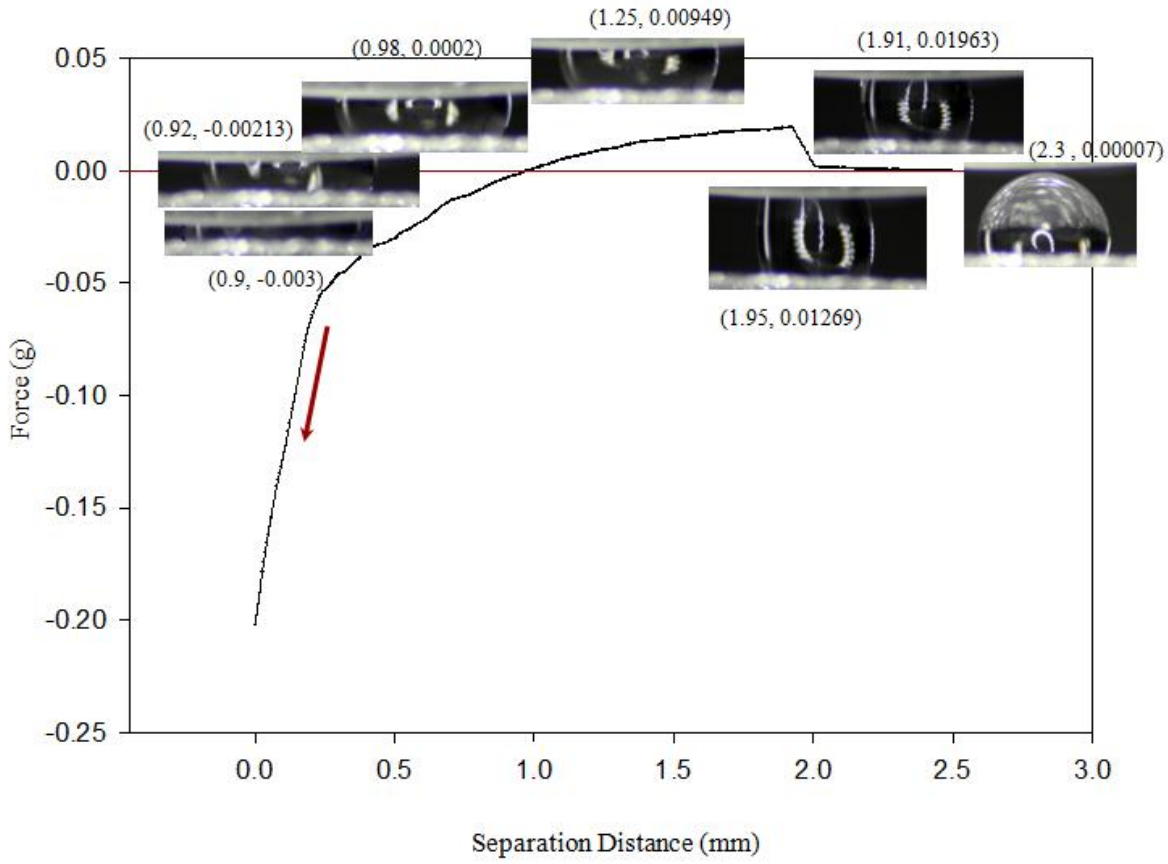

Figure 4.14. Curve depicts the first phase or force-application part of the robustness experiments.

The liquid drop is moved up once the distance between the two surfaces was set. The initial straight line in Figure 4.14 indicates the drop comes into contact with the upper Teflon® plate. The sharp increase in the curve at approximately 2 mm is due to the first contact of drop and upper plate. This is the point at which a capillary bridge-like formation appears. The increase in apparent weight or gram-force recorded on the balance is due to the attractive forces between the drop and plate. This attractive force increases due to the tension exerted

by the drop which pulls on the plate. The attractive force starts decreasing as the tension in the drop is relieved because the distance separating the two surfaces gets smaller. Force becomes insignificant at 0g, the critical point between repulsive and attractive force momentarily when the distance is sufficient to position the drop in its initial position before contact. This position is the point at which the drop might be under least tension. The plate then starts squeezing the drop, causing it to advance across the surfaces. When the compression of the drop begins, the contact angle remains static on the fabric while the contact angle on the Teflon® plate constantly advances, spreading over it. The droplet starts spreading across the fabric surface with decreasing distance between the fabric and the plate. Now, the repulsive force resisting further compression of the drop starts increasing. This force then decreases as the plate starts squeezing the drop causing it to advance across the surfaces. Spreading occurs with relative ease. Advancing of the drop occurs when the drop has been forced to attain its advancing contact angle. The resistive force then increases in the negative direction as the drop resists the force applied on it i.e. resistive force increases. This resistive force trend continues till the distance between the two surfaces becomes zero. The maximum force applied on the drop is obtained at this final point. At maximum compression, the drop's contact radius with the plate was equal to the drop radius. Excess force is required to cause penetration of the completely spread liquid film. There is difficulty in viewing the drop when the two surfaces are closed upon each other. The final applied weight at the point where the plate is completely pressed against the flat drop surface is recorded. The maximum pressure is buffered by the resistance offered by the liquid.

The drop of liquid at its maximum spreading coefficient may act as a buffer film. An observation made was the liquid drop being attracted to the Teflon® plate before contact with the surface. The Teflon® does not get close enough to touch the droplet; instead the drop rises to meet the Teflon® coating and wets it. This aberration may be due to charges accumulated in the Teflon® plate. In case of water, the drop is completely lifted off the fabric to the Teflon® and there is no contact with the fabric surface until the platform slowly rises to squeeze the drop against the plate. This occurrence is due to the fact that liquid droplet prefers the surface that is less hydrophobic, in this case, Teflon® plate.

4.2.2. Phase II: Force removal

The maximum compression is followed by removing the pressure applied. This involves the motor being reversed which causes the fabric to move downward. This motion increases the distance between the plate and the fabric causing the extraction of the imbibed liquid from the structure. It is termed as extraction due to the adhesive forces between the liquid and the Teflon® plate as well as between the liquid and the fabric (Figure 4.12 [g]).

During relaxation of the pressure, receding contact angles are observed once the drop is pulled out from within the fabric matrix. At this point, the fabric was lowered as is shown in Figure 4.15 while continuing to monitor the apparent weight of the plate. In this phase, the force required to dewet the plate from the droplet can be measured. As the fabric and drop were lowered, the drop pulled on the upper plate due to the force of adhesion, leading to an

increase in the weight and on lowering the fabric further, the drop eventually separated from the Teflon® coated aluminum (upper) plate.

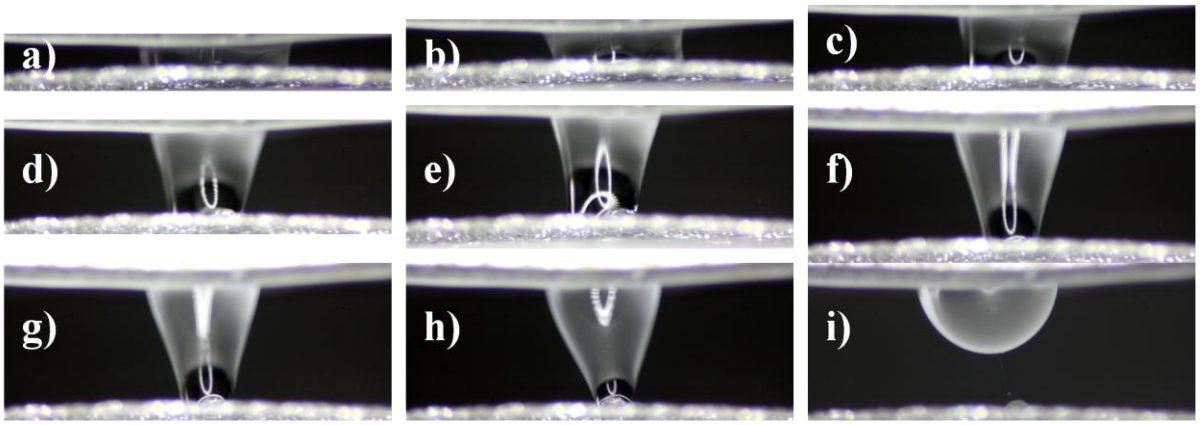

Figure 4.15. The force is being removed off the water drop on the fabric. The rupture of liquid between the two surfaces occurs gradually when the distance is sufficiently large.

Figure 4.15 shows the force decreasing as the surfaces move apart. The resistance offered by the suppressed drop decreases. At zero, there is negligible force acting on the drop as it is under insignificant tension. The force increases in the positive direction as the drop is pulled out from the fabric texture. The attractive force between the drop and the Teflon® plate increases due to the strong adhesion between the two. This causes the force to increase sharply. There is evidence of strong interaction between the liquid and the structure. The point where the force starts decreasing maybe due to the fact the drop that has now been pulled out starts receding along the plate after its receding contact angle had been attained. The force gradually decreases as the drop consistently receded on the plate and finally, the

capillary bridge breaks due to cohesive failure of the liquid. This break is denoted by the sharp dip in the curve towards the end of the decay.

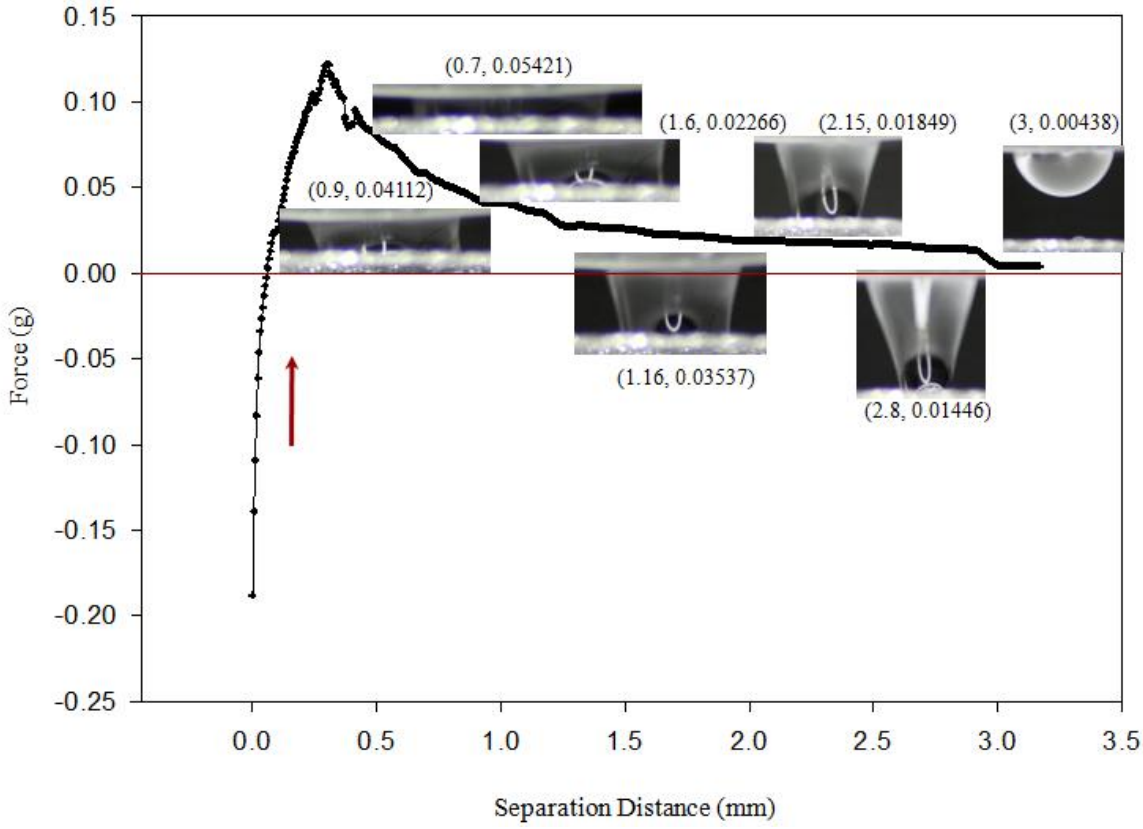

Figure 4.16. Curve depicts the second phase or force-removal part of the robustness experiments.

However, the force will not be zero due to the presence of the residual liquid on the Teflon® plate (Figure 4.16). This residue is due to the fact that Teflon® has a higher surface energy than the fabric and the contact angle of the drop on Teflon® is smaller than on the fabric

which makes it relatively more "philic" to the drop. Figure 4.17 shows the two curves discussed above in the single-cycle complete process. The curves override at certain points as the distance between the surfaces are the same and hence, the force on the drop is more likely the same. The hysteresis between the curves is due to the contact angle hysteresis. Also, the greater force is involved in extracting the drop from within the fabric texture. The sharp peak in the curve just before the drop is pulled out of the surface texture shows a stronger force is required to dewet the fabric. This implies a larger removing force than applying force. It is obvious that the shape of the drop after the application of pressure is clearly different than before applying the pressure.

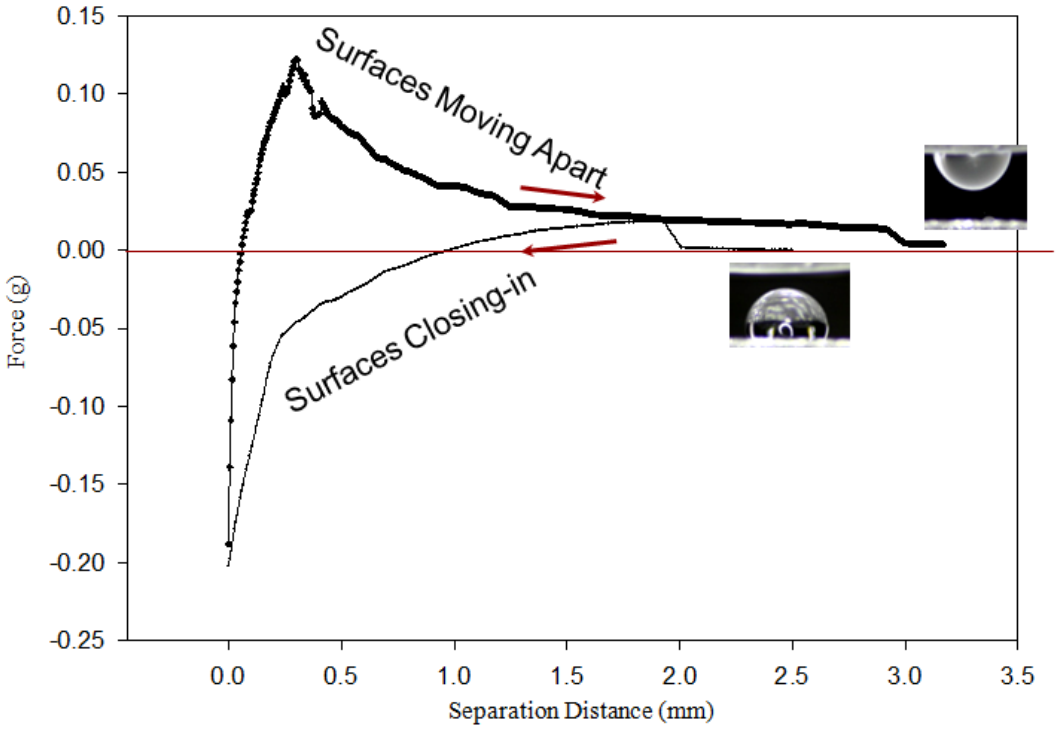

Figure 4.17. Curve shows the forces acting on a 10µl drop of water placed on a simple woven structure.

The experiment was repeated for Kaydol and dodecane droplets as well.

4.3. Observations

The contact angle increases initially when pressure is being applied and it decreases when the pressure is removed. Two conditions were observed:

With high surface tension liquid, the contact angle hystereses were observed to be similar before pressure application and after pressure relaxation, which revealed the transitions were reversible and hence, the superhydrophobicity/ superoleophobicity of the fabric was preserved. With low surface tension liquids, the hystereses before and after pressure were found to be very large, which showed that the transition was irreversible to the completely wet phase.

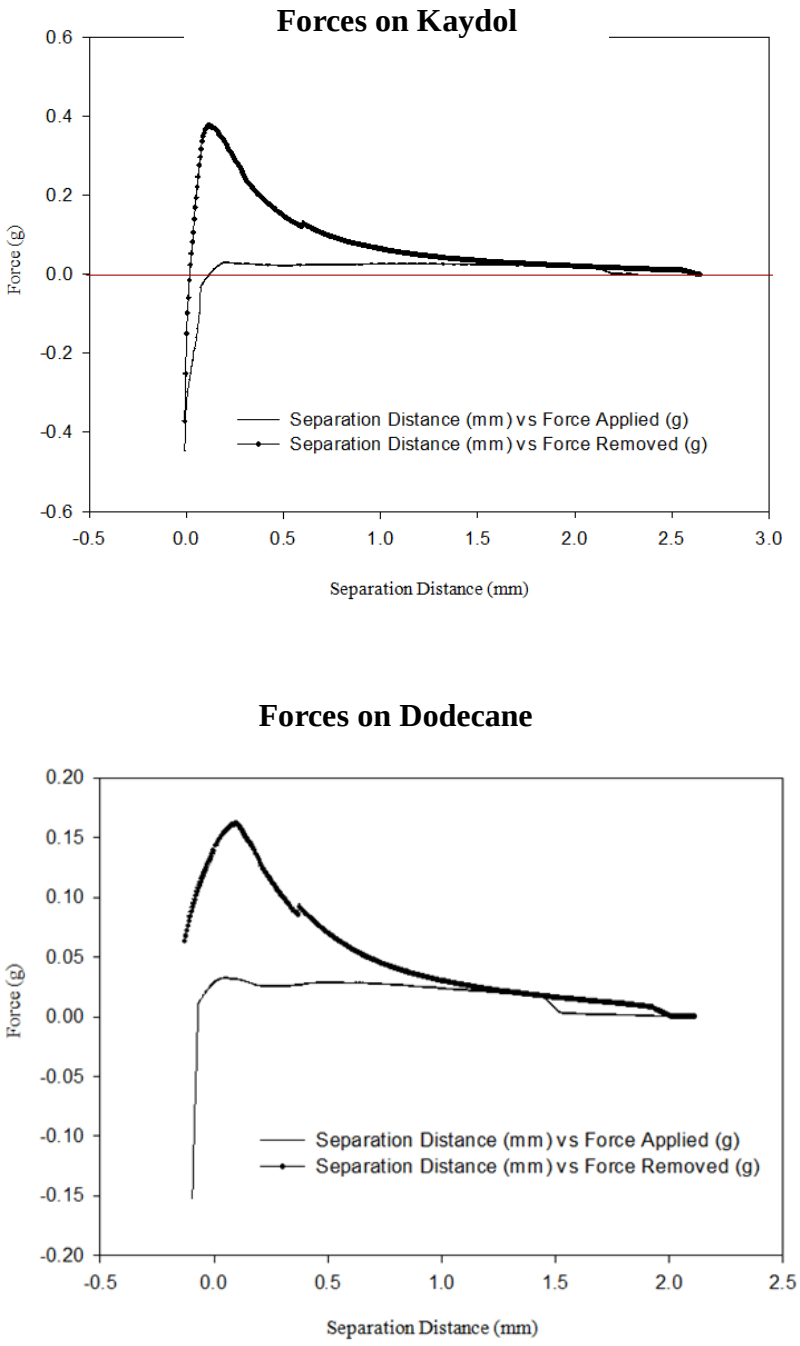

Figure 4.18. Curves show the forces acting on a 10µl drop of (a) Kaydol and (b) dodecane placed on a simple woven structure during compression and relaxation phases.

Figure 4.18 shows that there is significant hysteresis when force is applied and removed on Kaydol and dodecane droplets respectively. Moreover, the force required to pull Kaydol from within the surface is greater than that required for dodecane. This is evidently because of the easier spreading and penetration of Kaydol into the fabric texture than dodecane.

Liquid / Position	Water	Kaydol	Dodecane
Before Compression	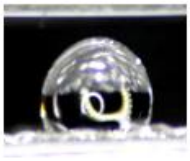	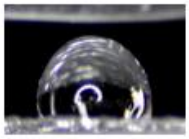	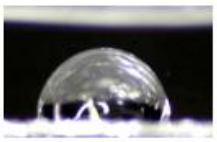
During Relaxation	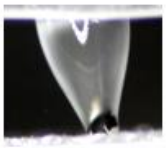	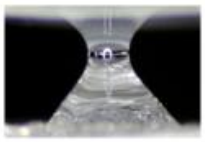	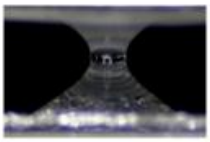
After Relaxation	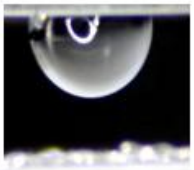		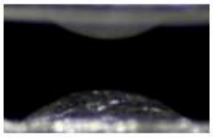

Figure 4.19. Images showing water and Kaydol drops before the robustness test (above) and the residual drops of the same on the fabric surface after force relaxation (below).

Figure 4.19 shows the amount of residue on the surfaces after the rupture of the capillary bridge. This determines if the fabric is dewet or partially wet. This depends on the interfacial energies, cohesion in the capillary bridge, adhesion between the liquid-solid, which can be

measured from the solid-liquid interfacial energy. The amount of air fraction also determines the amount of drop retained on the fabric after capillary break. Fluoro composition of surfaces lower the surface energy, but since Teflon® has a higher surface energy, it is more attractive to the liquid. Teflon® which exhibits the lower contact angle with the droplets will be more attractive.

In case of reversible transitions, after pressure relaxation, the Cassie-Baxter state is eventually recovered with less adhesion to the substrate. In contrast, for irreversible transitions, the receding angle is very small causing the liquid to be pinned to the structure (Figure 4.19). The pressure applied on the drop is almost the same as the Laplace pressure within the drop (which is of the order of 0.0102 g/mm^2 [10^2 Pa] 0.0102 g/mm^2 [10^2 Pa] for a millimeter fabric texture[28]). This emphasizes the instability of the meta-stable Cassie-Baxter state.

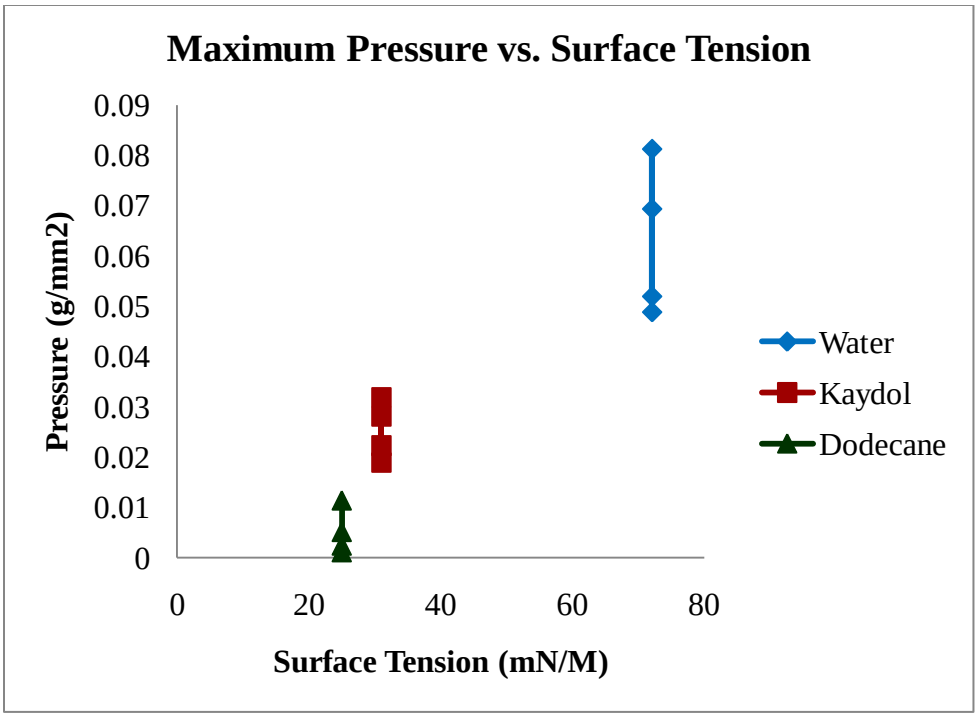

Figure 4.20. Pressure is observed to be a function of surface tension of the respective liquids.

From Figure 4.20 it is clear that water with the highest surface tension (72.8 mN/cm) requires the highest pressure to be pushed into the fabric. Also, surface tension determines the liquid spreading and the resistance that a liquid offers against the applied force.

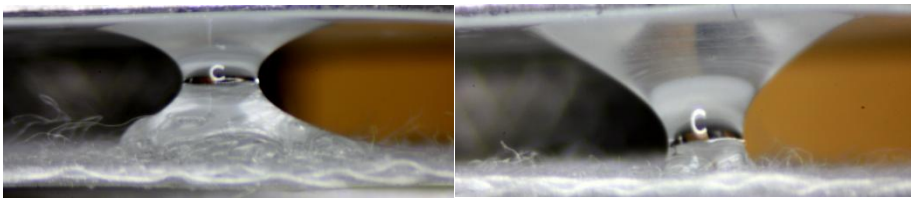

(a) (b)

Figure 4.21. (a) Dodecane and (b) Kaydol on perfluorinated cotton surfaces during the pull-off phase displaying the formation of capillary link and a flat film with a capillary connection.

As stated by Vagharchakian et al[54] at low pull-off velocities, a quasi-static regime is observed. When the applied weight on the droplet is being removed, the observed contact angle remains static initially as it remains energetically pinned to the fabric texture. This stage when the shape of the capillary link does not shift much is the quasi-static regime. Above a critical pull-off velocity, a dynamic recession of the drop is noticed. This is the point at which the inherent receding contact angle is attained and the receding contact angle starts decreasing rapidly. This is characterized by the stretching of the drop with a capillary link between the Teflon® plate and the fabric surface (Figure 4.21). The link is allowed to adjust as it is pulled apart between the plate and the fabric. The triple phase line at the solid-liquid-vapor interface moves all over the contact area on the fabric surface. Adhesive forces or wetting interactions tend to keep the liquid in contact with the fabric. The liquid-vapor interface at the capillary link decreases with increasing distance; it is this balance between the liquid-vapor interface and the liquid-solid-vapor regime that partly determines the shape of the drop after cohesive failure. The capillary link gets thinner with increase in the *z* direction, the central part thins down and it finally ruptures when the cohesive bonds are broken. The forces creating the capillary link oppose the adhesive forces on the fabric surface until the final rupture. Even if the force removal or the pulling- off stage is a slow quasi-static process, the breaking of the capillary link is highly unstable and occurs rapidly. Under the dynamic receding movement of the drop, noticeable deformations of the capillary link as well as the shape of the drop on the fabric surface occur. This results in a partial volume of the drop to be separated from the main volume and the drop remains attached to the upper

plate. The volume of this drop depends on the dynamic regime and is strongly affected by very small differences between the chemical treatments, vibrations in the air, mechanical disturbances of the Teflon® plate, possible contaminants in the Teflon® and the fabric.

Initial robustness tests were conducted on complex fabric structures in order to characterize the robustness experiments. Fluorosilane treated flame-retardant woven, knit and simple woven cotton samples were used. The contact angles and roll-off angles measured on these fabrics are tabulated in Table 4.2.

Table 4.2. Contact (10µl drops) and Roll-off Angles (50µl drops) Measured on Fluorosilane-treated Woven, Knit Fabrics

Sample	Liquid	Contact Angle	Roll-Off Angle
FR Woven	Water	158.2±2	21.2
	Kaydol	150.8±2	14.9
	Dodecane	131±2	26.7
FR Knit	Water	163±2	24.6
	Kaydol	149.4±2	16.3
	Dodecane	139±2	25.1
Cotton Woven	Water	153.2±2	24.6
	Kaydol	151.4±2	14.6
	Dodecane	134.9±2	27.6

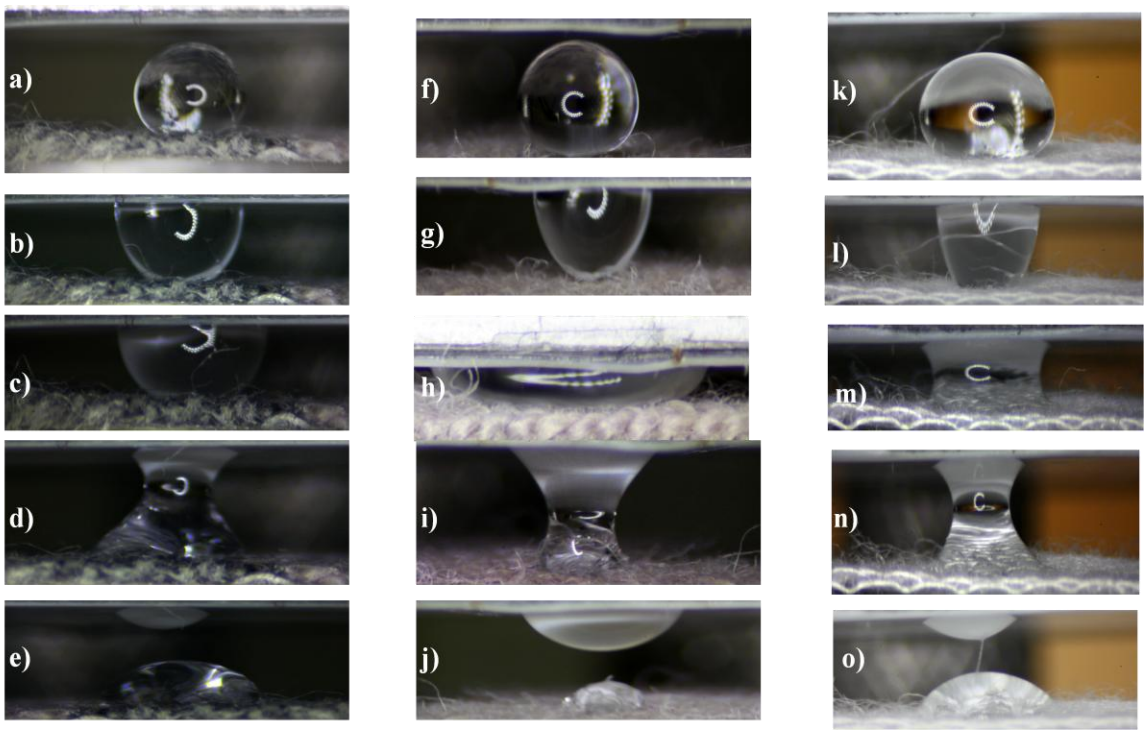

Figure 4.22. (a) Water droplet on FR rayon woven fabric. (b) Water drop in contact with the Teflon®-coated plate. (c) Droplet being squeezed. (d) Applied weight released. (e) Residual droplet on Teflon® after complete force removal. (f) Water droplet on FR knit fabric. (g) Water drop attracted to Teflon®-coated plate. (h) Droplet being squeezed. (i) Applied weight released. (j) Large drop volume preferred Teflon®. (k) Water droplet on treated cotton woven fabric. (l) Water drop forming a channel between fabric and Teflon®-coated plate. (m) Droplet being squeezed. (n) Applied weight released. (o) Droplet preferred fabric.

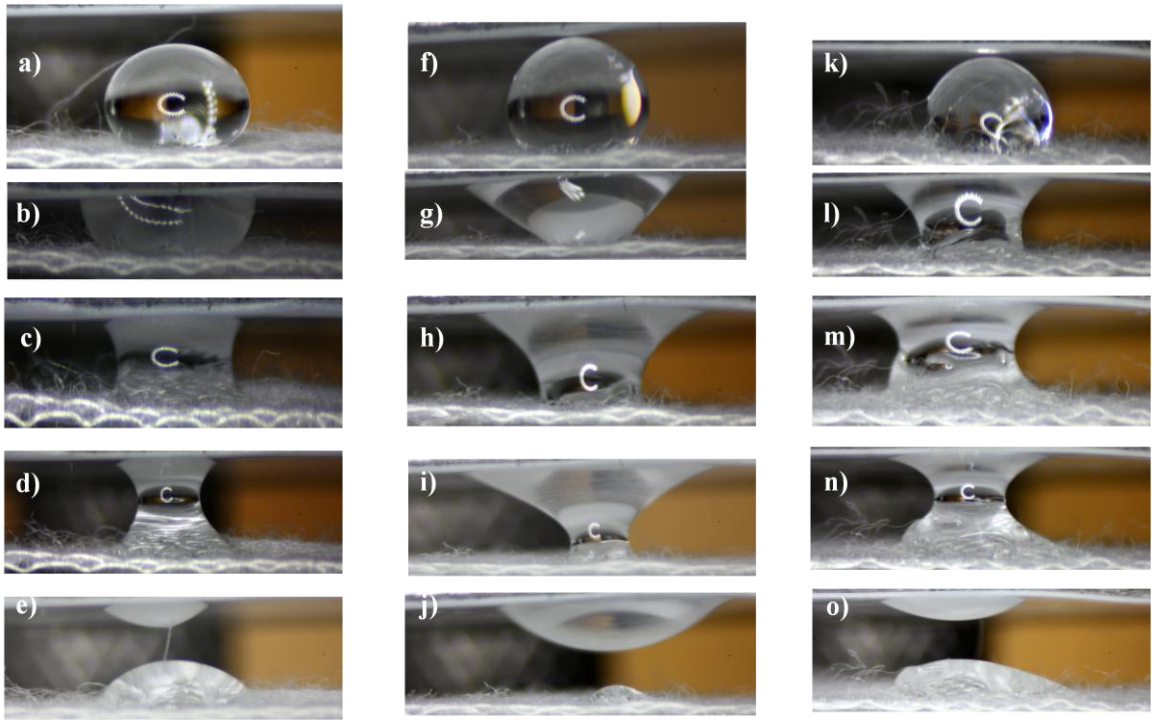

Figure 4.23. Robustness measurements made on a water/ oil-repellent cotton woven fabric with 10 µl each of liquid (a) Water on fabric. (b) Pressure applied by plate on drop. (c) Pressure released on drop. (d) Extension of drop with withdrawing plate. (e) Partially wet fabric. (f) Kaydol droplet on fabric. (g) Kaydol attracted to Teflon®-coated plate. (h) Pressure removal on Kaydol. (i) Film formation on Teflon® plate. (j) Large drop volume preferred Teflon®. (k) Dodecane on fabric. (l) Dodecane being squeezed. (m) Plate receding from drop. (n) Symmetric capillary channel formation. (o) Completely wet fabric.

Table 4.3. Robustness Pressure Measurements

Sample	Liquid	Force (g)	Area (mm^2)	Pressure (g/mm^2)
FR Woven	Water	0.6	50.24	0.0119
	Kaydol	0.526	50.24	0.0104
	Dodecane	0.472	78.5	0.006
FR Knit	Water	0.9	50.24	0.0179
	Kaydol	0.2656	63.58	0.0041
	Dodecane	0.14	78.5	0.0017
Cotton Woven	Water	0.3615	38.46	0.0094
	Kaydol	0.3002	94.98	0.00316
	Dodecane	0.3595	50.24	0.00716

Note: Force is taken to be the negative of the apparent weight in grams.

In Figures 4.22 & 4.23, it can be seen that the liquid breaks in a different manner for the different fabrics and different surface tensions of liquids. After the liquid breakage, a droplet is mostly retained on the fabric (as in Figure 4.22, water and dodecane on cotton woven fabric) as compared to Kaydol on cotton woven fabric, on which most of the droplet is on the plate. The time taken for breakage to occur depends on the contact angle hysteresis. The

higher the contact angle hysteresis, the longer and slower is the process. A lower contact angle ensures swift retraction of the liquid on either the fabric or the Teflon® plate and quick liquid rupture.

Although the 3 different fabrics (woven, knit, cotton woven) in Figure 4.22 have the same superhydrophobic/ superoleophobic surface treatment, their wetting behaviors differ significantly from the observations based on the liquid profiles during force application and force removal. From Table 4.3, Kaydol is shown to have a lower contact angle hysteresis (roll-off angle) than water or dodecane despite having an intermediate surface tension of 31 mN/m. The residue of Kaydol is larger on the Teflon® after plate separation because, the drop spreads more than the other two liquids and hence it forms a buffer film on the surface. It can be said that the maximum applied pressure is not sufficient to cause the Kaydol to transcend the surface and traverse the fiber structure. It is because Kaydol will not be completely pushed into the fabric due to the excessive spreading that when the plate is slowly pulled-off the drop, the liquid easily gets attracted to the less hydrophobic and oleophobic surface (i.e. Teflon®) and hence the subsequent larger volume of droplet on the Teflon® plate as compared to the other two cases. Kaydol functions as a buffering layer between the fabric and Teflon® surfaces, supporting the weight of the Teflon® plate. Also, the volume of the drop on the fabric also depends more on the receding contact angle than the static contact angle. Variations in the velocity of the experiment will also affect the volume and shape of the drop. Vagharchakian et al[54] have demonstrated that the wetting behavior is affected

differently by high and low velocities of withdrawing a surface from a liquid. The speeds determine the amount of liquid retained on the surface after the contact area has been removed from the liquid. High velocity pull-off leads to retention of a larger volume than at low velocities.

Table 4.4. Calculated Robustness Pressures vs. Measured Breakthrough Pressures

Liquid	Diameter (mm)	Area (mm^2)	Applied Weight (g)	Predicted Breakthrough Pressure (Pa)	Measured Maximum Pressure (Pa)
Water	3.2	8.11	0.49	0.372	0.062
Kaydol	4	12.66	0.31	0.069	0.025
Dodecane	5.1	21.05	0.11	0.03	0.004

Table 4.4 shows that although the maximum pressure measured on the robustometer is not as large as the theoretical values, there is significant breakthrough. However, water-tested fabric remained dewet indicating the robustness of the fabric at the the maximum applied pressure. This is not necessarily the robust pressure. In earlier findings, the depth of penetration of the liquid drop was found to be approximately 0.5 mm for all the three drops under pressure. It has to be noted that the thickness of the fabric is only 0.18 mm. This is indicative of the fact

that the fabric sags between its clamped ends on the metal stage and a reservoir is formed when the liquid is pushed on the fabric and hence the reason for the penetration depth being substantially greater than the thickness of the fabric. The fiber spacing is 0.13 mm (130.3 μm). In theory, $2d \approx$ fabric thickness, h; this would be a potential cause for considerable liquid sag to cause failure of the composite regime.

The diameter of the fibers is measured using analysis of photos on ImageJ software. The area of contact of the droplet with the fabric at maximum compression is a circle and the radius is measured using a photograph of the compressed droplet with a two dimensional millimeter ruler. The depth of penetration of the liquid into the interstices of the fabric is obtained from:

$$V = A \times h \tag{4.5}$$

where, V is the volume of the droplet, A is the area of contact, and h is the depth of penetration.

The weight applied on the droplet is that which has been recorded from the analytical balance. This is the measure of force acting on the drop. It has to be noted that as the force increases, the weight recorded is negative. Measured maximum pressure is the pressure at which the radius of the drop is measured. The radius is measured using a ruler in two dimensional planes. This depends on the level of visibility and it is recorded as close to the maximum compression as possible. At this point, the drop is usually completely spread over

the surface. The recorded units are in g/mm^2 which is converted to Pascal for convenience. The predicted breakthrough pressure is that which has been calculated based on equations for robustness in literature.[48] The calculated pressures for the plain woven nylon fabric are much higher than those that were measured. This is a clear indication that the pressure required to cause penetration to the wet phase is much smaller than theoretical predictions. This is due to the fact that robustness values differ with structures.

Also, in terms of spacing ratio for the simple woven structure,

$$D^* = \frac{d + R}{R}$$

For $2d$ = 130.3μm and R = 68.2 μm, D^*= 1.95. Although, $D^*$was found to be higher, the robustness of such a fabric was poor. There is a trade-off between the adjacent fiber spacing and the pore depth of the fabric; greater the distance between two fibers, the better the contact angles, but beyond a critical value of $2d$, the curvature of the sagging liquid might be as large as the fabric thickness to cause failure of the composite regime.

Robustness is a measure of the mechanical stability of a textile material to resist external forces that aim to deform and destroy the solid-liquid-vapor interface when a droplet is perched atop a protrusion and air space. A robust composite interface is required to support oleophobicity and this depends on the surface geometry, equilibrium contact angles, and liquid properties, especially surface tension. Lafuma and Quéré[28] reflected that a robust

surface is one that should be able to support droplets in the stable Cassie-Baxter state even when the internal pressure of the drop causes the liquid meniscus to inch closer to the substrate between the protrusions. In regards to this, increasing the height of the protrusions might be a good alternative to wetting .[56] A liquid with higher surface tension would spread much less on the surface and offer a greater resistance to the robust pressure that causes it to be forced into the fabric.

The robustometer helps in the measurement of the breakthrough pressure required to push a droplet of a liquid into a given superhydrophobic or oleophobic sample in order to determine its robustness. This also helps measure the force that is involved in transferring a drop from its meta-stable Cassie-Baxter state to complete wetting (or not, in the case of a robust rough surface). The contact area of the drop was also simultaneously observed and thus, the maximum pressure taken to push a drop into the fabric was measured. This breakthrough pressure evaluation gives an estimation of the robustness of a surface that helps in modeling a surface that would allow maximum stability of a composite interface of oil-solid-air. This not only gives a measure of the maximum robustness pressure, but also indicates if a fabric is wetted or de-wetted.

4.4. Change of free energy

To elucidate the transition from the meta-stable Cassie-Baxter state to the Wenzel state due to the downward propagation of the liquid-vapor interface, the variation in the specific

Gibb's free energy on different location of the rough surface needs to be calculated. When the drop of liquid is squeezed between the plate and the fabric, the drop initially offers resistance to the force acting on it. The drop spreads on the fabric surface in a circular area of contact due to surface tension which counteracts the force causing distortion of the drop circumference. As the drop spreads, interfaces are created and destroyed. After a critical force, the drop stops spreading as it gets pushed into the fabric structure. It gets pushed to a certain depth determined by the fabrics' characteristics and its robustness. The activation energies of the process responsible for spreading and penetration are greater for penetration than spreading as a higher energy barrier has to be overcome to cause the Wenzel transition. As the drop moves over and into the fabric, a solid-vapor interface of area, A_{SV} is destroyed and an energy, $\gamma_{SV} \times A_{SV}$ is gained, where γ_{SV} is the solid-vapor interfacial energy; an energy $\gamma_{LS} \times A_{SV}$ is expended in forming the liquid-solid interface over the same area, where γ_{LS} is the liquid-solid interfacial energy. Marmur showed that the stability of a composite interface can be predicted by computing the Gibbs free energy, *G*. The Gibb's free energy, in forming the geometrical area of the interface, assists in understanding the transition from heterogeneous to homogeneous wetting regimes. The total energy of the system is calculated as a sum of the contact surface areas times the surface energies.

$$G = \gamma_{LV} A_{LV} + \gamma_{LS} A_{LS} + \gamma_{SV} A_{SV} \tag{4.6}$$

Equation 4.6, due to the creation new liquid-fabric interface, becomes

$$G = \gamma_{LV} A_{LV} + \gamma_{LS} A_{LS} - \gamma_{SV} A_{LS} \tag{4.7}$$

From *Dupré -Young's* Equation,

$$G = \gamma_{LV} (A_{LV} - A_{LS} \cos\theta_e) \tag{4.8}$$

The force, *F*, required to form unit area of the interface is

$$F = \frac{dG}{dz} = \gamma_{LV} (-\cos\theta_e \frac{dA_{LS}}{dz} + 2\pi \frac{dR_{\text{drop}}}{dz}) \tag{4.9}$$

which is correlated to the equation of a straight line with negative slope, comparable to the straight lines in the force application curves above,

$$F = mx + c$$

When the radius of the drop stops changing,

$$c = -2\pi R_{drop}$$

This is the point at which the drop stops spreading and gets pushed into the fabric. Although, the liquid-vapor interface is changing, there will be no change in the curvature of the liquid.

For the creation of a stable composite interface on any rough surface requires a local minimum in the overall free energy diagram and $dA_{LS}/dz < 0$.

4.6. Verification of robustness

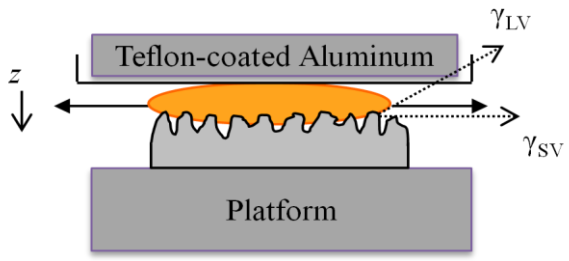

Figure 4.24. Distortion of a drop.

Figure 4.22 shows the deformation of small drops is contributed to surface effects rather than gravity.[11a] The curvature of the drop is determined by the Laplace pressure within the drop.[57] There two different surface tensions acting on the drop to maintain its curvature i.e. the one along the *z* direction, pushing the droplet inside the fabric and the one acting on the sides of the drop, spreading it across the surface. The change in curvatures of the droplet under deforming forces strikes a balance between the fabric and liquid interfacial energies i.e. γ_{SV} and γ_{LV}. However, interfacial energies do not change much with small pressures; although the contact angles change to accommodate forces to retain the curvature. In other words, surface distortion occurs to maintain constant γ_{SV} and γ_{LV}. Radius changes of the droplet curvature occur as the drop spreads and this is more evident than the deformation of the shape of the curvature. The surface tensions remain independent of the change in liquid-solid contact area.

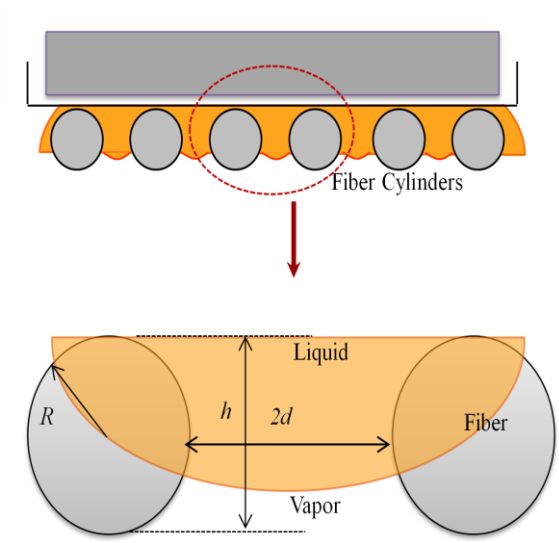

Figure 4.25. Changing interfaces under pressure.

Figure 4.23 represents a typical 10 µl droplet being forced between the fiber structures under robust pressure. The robustness of the fabric can be estimated from the volume of liquid present in the fabric interstices under pressure.

$$h = \frac{V}{A} \tag{4.10}$$

When a droplet of volume V is forced into the interstices of a fabric at the contact area, A, it penetrates to a depth, h which is determined by the height of the fiber. If this depth, h is in the same range as the fabric thickness, then there would be an estimate to calculate the depth of liquid penetration into the fabric structure.

This could be correlated to the total volume of interfacial area that is wetted by the liquid when it is under the influence of robust pressure as shown in Figure 4.27:

$$V_{total} = A_w \times t_w = V_f + V_l + V_a \tag{4.11}$$

A_w is the area that is wet by the liquid, t_w is the thickness of the wet area, V_f is the volume of the fiber portion that is wet, V_l is volume of the liquid penetrating the fabric, and V_a is the volume of the air space between the wet fibers. Area of the wet interface can be obtained from $A_w = \pi R_{drop}^2$. Volume of fibers in the wet interface can be calculated as follows:

$$V_f = V_{total} \times \text{solid fraction} \tag{4.12}$$

$$\text{Solid Fraction} = \frac{\text{Fabric Weight} \times \text{Fabric Thickness}}{\text{Fiber Density, } \rho_f} \tag{4.13}$$

$$V_a = (A_w \times t_w) - V_f - V_l = V_{total}(1\text{- solid fraction}) - V_l \tag{4.14}$$

If $V_a > 0$, then it indicates the presence of air in the wet space between the fiber spacing. Hence, there is an evident presence of air beneath the liquid which implies that the liquid penetration has not traveled the complete thickness of the fabric thereby causing complete wetting. Furthermore, if the liquid reverts to its original shape atop the fabric as it was before robust pressure application, it would go on to reiterate the robustness of the oleophobic surface. In most cases, the liquid droplet has better affinity to the Teflon® plate

than to the fabric and hence there is more effort involved in climbing onto the Teflon® rather than penetrating the fabric. This is essentially due to the presence of air pockets under the drop that causes it to prefer the less hydrophobic Teflon® surface.

This volume measurement was used as a preliminary evaluation which led to the discovery of fabric sagging under pressure. The robustness of the fabric can be estimated from the volume of liquid present in the fabric interstices under pressure.

4.7. Scope of the robustness test using robustometer

This test method is used to evaluate the resistance of materials used in protective clothing to penetration by liquid drops under conditions of continuous liquid contact and increasing direct mechanical pressure. The penetration resistance of fabrics is based on visual detection of liquid penetration at a specific applied mechanical pressure. Fabric wetting or dewetting and therein, the degree of robustness of the fabrics are based on visual detection of liquid

penetration. The fabrics considered are treated or modified to repel liquid. The degree of robustness is therefore more a function of repellant quality and the surface tension of the liquid under test.

Part of the protocol in the procedure is for exposing the fabric to 10µl liquid droplets subject to small pressures. This maximum pressure has been documented to discriminate between performances and correlate with visual penetration results that are obtained with human

validation. The breakthrough pressure (P_H) calculated from literature[48] suggests that mechanical pressures greater than those measured can occur. Therefore, it is important to understand that this test method does not simulate all the physical stresses and pressures that are exerted on protective clothing garments during actual use. This test method is offered to identify those protective clothing materials that warrant further evaluation with a technological challenge.

Based on visual observations of wetting and dewetting alone, this test method can be used as a preliminary evaluation for possible penetration of high and low surface tension liquids. Robust pressure varies with different fabric structures for different liquids. The differences in chemical and molecular properties (for example, surface tension) of liquids lead to different results. Surfaces which can resist low surface tension liquids such as dodecane (25 mN/m) are rare. This method will not apply to all forms or conditions of liquid penetration, but only for those that are not affected by the hydrostatic pressure. The robustometer can demonstrate the robustness of any fabric including those that are impacted by storage conditions and shelf life, and laundered and sterilized reusable ones. The robustometer identifies if the integrity of the superhydrophobic and superoleophobic fabric has been compromised during use by such effects as flexing and abrasion. The robustometer also addresses the design and overall construction of the fabric. It could aid in the evaluation of the barrier effectiveness against liquids of materials used for protective clothing and not for finished items of protective

clothing like whole garments or garment parts. Reviewing the mode of work or clothing exposure and assessing the appropriateness of this test method for specific applications would be recommended. It is also possible to use this test method as a material quality control or assurance procedure.

4.8. Limitations and recommendations

There are some limitations or factors based on the design of the robustometer. There are factors that need to be taken into further consideration as the robustometer is still in its developmental phase and hence, there might be fluctuations in measurements and subsequent analysis. The observations made on the robustometer could be erroneous for the same reason.

All the observations made on the robustometer were manually read which poses a constraint on time and accuracy. This can be rectified by connecting a load cell to record the applied weight and displacement. Automating image capturing could aid fasten the process.

The kinetics of motion of small liquid drops was qualitatively observed. Their wetting behavior elicits exact dynamic measurements of advancing and receding contact angles, measurement of contact areas which are tedious to record. A microscope can offset the problems with viewing the changing surface curvature of the drop under pressure.

One of the potential problems arising was mechanical sagging of the front edge of the fabric positioned on the U-shaped opening of the metal platform. This led to incorrect force recordings. The depth of penetration of the liquid was higher than the fabric thickness for the

same reason. This can be avoided by using a thin wire mesh support under the fabric. The sagging causes the liquid to be logged in a reservoir when the upper plate is compressing upon the fabric at maximum applied weight.

It is also possible that pre-wetting by contaminating materials such as alcohol and perspiration can also compromise the integrity of the results. An appropriate preconditioning technique can be employed to avoid such errors, such as cleaning the Teflon® plate with methanol for every repeat of the experiment and usage of a new sample.

Chapter 5 Conclusion

Understanding the ability of a liquid drop to dewet the fabric surface on removal on any external force placed on it can provide basic information about the durability of superoleophobic or self-cleaning materials. The development of the robustometer contributes to the same. In essence, a quantitative measure of determining the robustness of a surface was introduced in this research.

This methodology is of significance due to the fact that the hydrostatic head pressure has insufficient influence over small droplets. It was found that small droplets did not penetrate a rough surface under small pressures, but rather spread out significantly along the surface (Figure 5.2). However, with sufficient pressure supplied to the system, penetration of the liquid occurred. The drop was found to deform and change shape considerably. The fabric tried to keep the liquid out from imbibitions for an initial period of time which was evident from the droplet spreading rather than sinking into the structure. When pressure was released, it was often noted that a certain amount of liquid transferred to the Teflon® surface. This could be in effect due to the type of liquid used, the speed of retraction of the plate from the droplet, charged contaminants on the plate, etc.

On release of pressure, two possibilities arose:

1. The liquid droplet pulled back up to the surface, indicating a significantly robust superhydrophobic and superoleophobic surface.

2. The liquid fails to resurface and remains embedded in the fabric structure, indicating a complete wet surface with inadequate robustness (Figure 5.1).

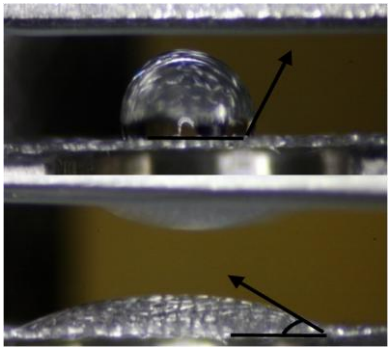

Figure 5.1. The change in contact angles before and after pressure application (above) and removal (below) indicate that the 10 µl dodecane drop after pressure removal completely wets the fabric signifying low robustness of the surface.

From the shape of the capillary link during force release and drop extension and the force observed on the analytical balance, stress-strain curves can be obtained. The resistance offered by the liquid to deform can be observed on such curves.

Figure 5.2 demonstrates that the droplet does spread across the fabric substantially. This is relatively reproducible in actual practice. Since this is the first effort at the instrumentation of the robustometer, it inevitably has a few limitations such as the fabric deforming to form a sagging curvature which can provide a reservoir to the drop under pressure. The Teflon® coated aluminum plate did not always remain planar under dynamic drop movement.

Figure 5.2. Image (left) shows a thin film of dodecane between the Teflon® coated aluminum plate and fabric. Cartoon (right) depicts the same of the small deformed drop of dodecane.

Thus, the robustometer was constructed and tested for behavior of liquid repellent fabrics subjected to small drops under robust pressure. The degree of robustness of the fabric determined the range of super-repellent property of the fabric. Wetting and dewetting observations were made. Certain shortcomings were identified and recommendations for improvement were made.

The most important of the recommendations that can be effected is supporting the fabric in order to eliminate the sagging of the structure. Fabrics are deformable and there is a greater tendency to deform under pressure and the effect is pronounced in light-weight fabrics. Hence, this is an issue that needs due consideration. If the fabric was supported on a smooth hydrophilic or oleophilic surface such as glass or untreated nylon, sagging of the fabric would be eliminated and the drop would have to traverse either a horizontal or vertical path. If the composite interface failed under pressure, the supporting substrate would give a clear indication of wetness.

Standard test methods which measure the barrier properties of textiles vary with the liquids used, the area of fabric in contact, and the amount and type of pressure applied. The robustometer can be used with any liquid or fabric.

The versatility of this test in characterizing fabric surfaces can be exemplified by a comparison between different perfluorinated fabric surfaces with different fabric constructions, ranging from the simple plain weave to the complex multi-layered woven fabric.

In summary, the robustometer has proved that a 10 µl droplet of liquid when subjected to external pressure spreads over a fabric surface forming a thin film before penetrating into the structure. The pressure required to trigger spreading and imbibitions is smaller than the hydrostatic pressure and the predicted breakthrough robust pressure. This is of prime importance while testing functional fabrics that protect against penetration by toxic substances that are lethal at volumes of 1 µl.

Chapter 6 Test Design and Development

In developing new high-tech textile products, there will be a constant challenge in testing the authenticity of the proposed technology. New materials and designs with novel functionalities elicit the need for simulating and designing testing procedures. For high-performance products, new methodologies of testing and validation should fit easily into existing testing technologies. Therefore, new product development often uses modifications of generic products and processes to easily access the potential markets.

6.1. Existing repellency testing

Repellency finishes are important components of many protective textiles. Applications for finishes range from medical to military. Most of the penetration tests involve hydrostatic techniques. Liquid is contacted with the material specimen and at least some portion of the specimen with the liquid is under pressure (Raheel, 1996).[58]

The American Association of Textile Chemists and Colorists **(**AATCC) Test Method 127-2008[59] is the standard for water resistance and hydrostatic pressure test developed in 1968. This test method measures the resistance of a fabric to the penetration of water under hydrostatic pressure. It is applicable to all types of fabrics, including those treated with a water resistant or water repellent finish. Water resistance depends on the repellency of the fibers and yarns, as well as the fabric construction. The hydrostatic pressure depends on the fabric construction and finish. It is a good indication of rain repellency.[60] AATCC Test

Method 22-2001 is a simple test for rapid screening of water repellency.[59] AATCC Test Method 35-2000 is designed to simulate a rain event. The water sprayed is under hydrostatic pressure with a blotter under the fabric. The blotter is weighed after the test to determine the percentage of water penetration through the fabric. ISO 9865 is a more severe rain simulation test. The fabric is rubbed on the underside during the water spray. The amount of water absorbed and the fabric wear are all factors in determining the repellency rate of the fabric.Oil repellency can be evaluated by AATCC Test Method 118- 2002. Drops of hydrocarbon with various surface tensions are applied to the fabric and the degree of wetting is determined. The fabric is assigned a repellency rating based on the hydrocarbon with the lowest surface tension that does not wet the fabric. INDA, the Association of the Nonwoven Fabrics Industry employs a repellency test specifically designed to evaluate a nonwovens's ability to resist gravity-only penetration by a saline solution. Another INDA test that is useful for medical applications is IST 80.8 (01). A series of liquids are placed dropwise on the sample to determine at what point the sample is wetted. The liquid used have varying compositions of water and alcohol.[61] Liquid permeability tests that are currently in practice determine the repellency of liquids by fabrics under the influence of gravity. For certain applications such as in the toxic chemical industry, the amount of liquid that can cause toxic effects if it penetrates the surface of the fabric to reach the epidermis is as small as 1 µl. With some toxic chemicals, this would prove fatal. The hydrostatic pressure is not applicable for such small droplets because of the insignificant gravitational force acting on them.

Wenzel pointed out back in 1936[7] that hydrostatic pressure testing is inadequate when comparing two different fabrics with the same superhydrophobic/superoleophobic finish because of the difference in their thread dimensions and air porosity (Wenzel, 1936). Hydrostatic pressure is influenced by the mechanical strength and uniformity of the fabrics.

Some of the test methods like the ASTM F1670 – 08, Standard Test Method for Resistance of Materials Used in Protective Clothing to Penetration by Synthetic Blood[62] and ASTM F903 – 10, Standard Test Method for Resistance of Materials Used in Protective Clothing to Penetration by Liquids[63] involve a qualitative determination of the protective clothing material resistance to penetration by synthetic blood or other liquids under specific test conditions, the robustness test gives a quantitative measure of the wetting behavior along with a visible evaluation.Majority of industry penetration tests are designed for use with water. Most of the devises cannot be used with other liquids or may even be damaged if water is not used.[58] Most of the existing standards employed up to 13.8 kPa of predominantly hydrostatic pressure to the liquid and the fabric. In operating rooms, the maximum pressure of blood reported has been 399.9 kPa and that 88% of the time pressure on impact was 20 kPa (2.04 g/mm^2) or less. For small liquid drops the pressure would be much lower and in such instances, the hydrostatic pressure test will prove to be inadequate. The primary tendency of such small droplets is to spread rather than penetrate.[64] This would require a new test method for exposure to liquids under extremely small mechanical pressures.

6.2. Product Innovation Charter (PIC)

Product Innovation Charter is a summary strategy that serves as a guide for generation and development of new product ideas. The product summary of the robustometer is encapsulated in Figure 6.1.

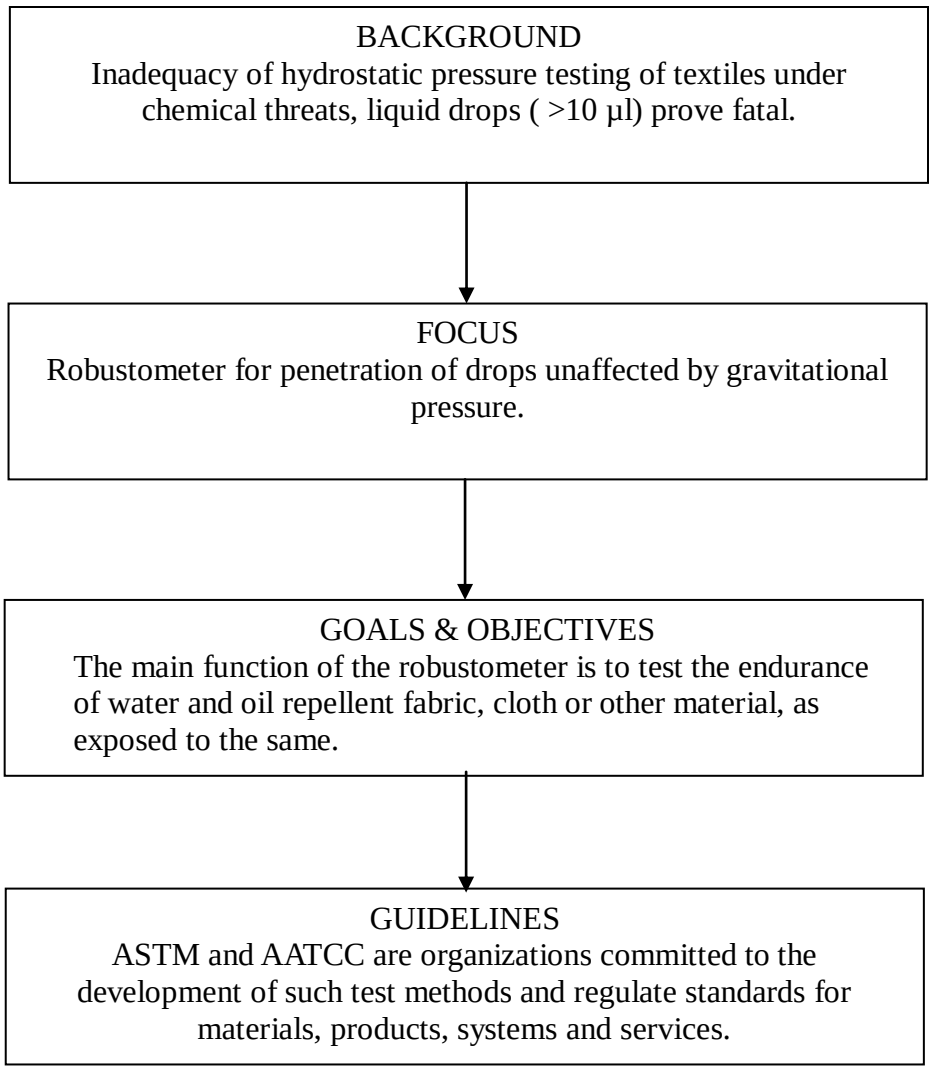

Figure 6.1. Product Innovation Charter for “robustometer”.

6.2.1. Background

For protective textiles that are used in surgery, military combat uniforms, farmers working with pesticides, and ship hulls, it is required that they be tested for the repellency of liquids of high and low surface tensions and large and small volumes. The amount of penetration has to be evaluated. In case of military use, tests would be required to give an estimate of dermal exposure to toxic contaminants and to evaluate the transfer of such chemicals to the clothing and skin upon exertion of crawling pressures of the elbow and knees.

Present testing methods like the AATCC Test Method 118-1992: Oil Repellency: Hydrocarbon Resistance Test and Alcohol Repellency Test Method (INDA 1ST 80.6-92) evaluate the resistance of fabrics to wetting by hydrocarbons (over a series of low surface tensions from 19.8 to 31.2 mN/m) and alcohols. The liquids are placed on the fabric and observed for wicking, wetting and penetration and graded based on numerical scales.[65] These are subjective evaluation methods.

6.2.2. Focus

Presently, there is no published work on quantitatively analyzing the robust breakthrough pressure. In order to characterize fabrics based on the robustness of their superhydrophobicity and superoleophobicity, a quantitative analysis of the pressure causing wetting by liquids with different surface tensions is proposed. This relies on the penetration of a liquid drop and the ability of the fabric texture to push it back to the surface. The test is carried out under controlled pressure.

6.2.3. Goals-Objectives

The goals and challenges for this study are to study and research various existing test methods that can be used to evaluate the penetration of liquid droplets through fabrics, develop the robustometer which evaluates the re-entrance capability of a liquid on a imbibed in a fabrics, and investigate testing methodology to facilitate the commercial viability of instrumentation of the working model of the robustometer.

6.2.4. Guidelines

The American Association of Textile & Colorists, AATCC and American Society for Testing and Materials, ASTM are non-governmental organization committed to the development of test methods and voluntary standards for materials, products, systems and services. The proposed robustness pressure test has to be designed and developed in accordance with the AATCC and ASTM guidelines. Some of the standards that would require adherence would be:

ASTM F 1670[62]

ASTM Standard Test method for Resistance of Materials Used in Protective Clothing to Penetration by Synthetic Blood. This test method is not designed to test the bioactive qualities of fabrics, but the physical qualities of the fabric.

ASTM F 1819

Standard Test Method for Resistance of Materials Used in Protective Clothing to Penetration by Synthetic Blood Using a Mechanical Pressure Technique, uses mechanical pressure as opposed to hydrostatic pressure to simulate the leaning and pressing that may occur during surgery. This test is quantitative and determines the penetration pressure of the test material.

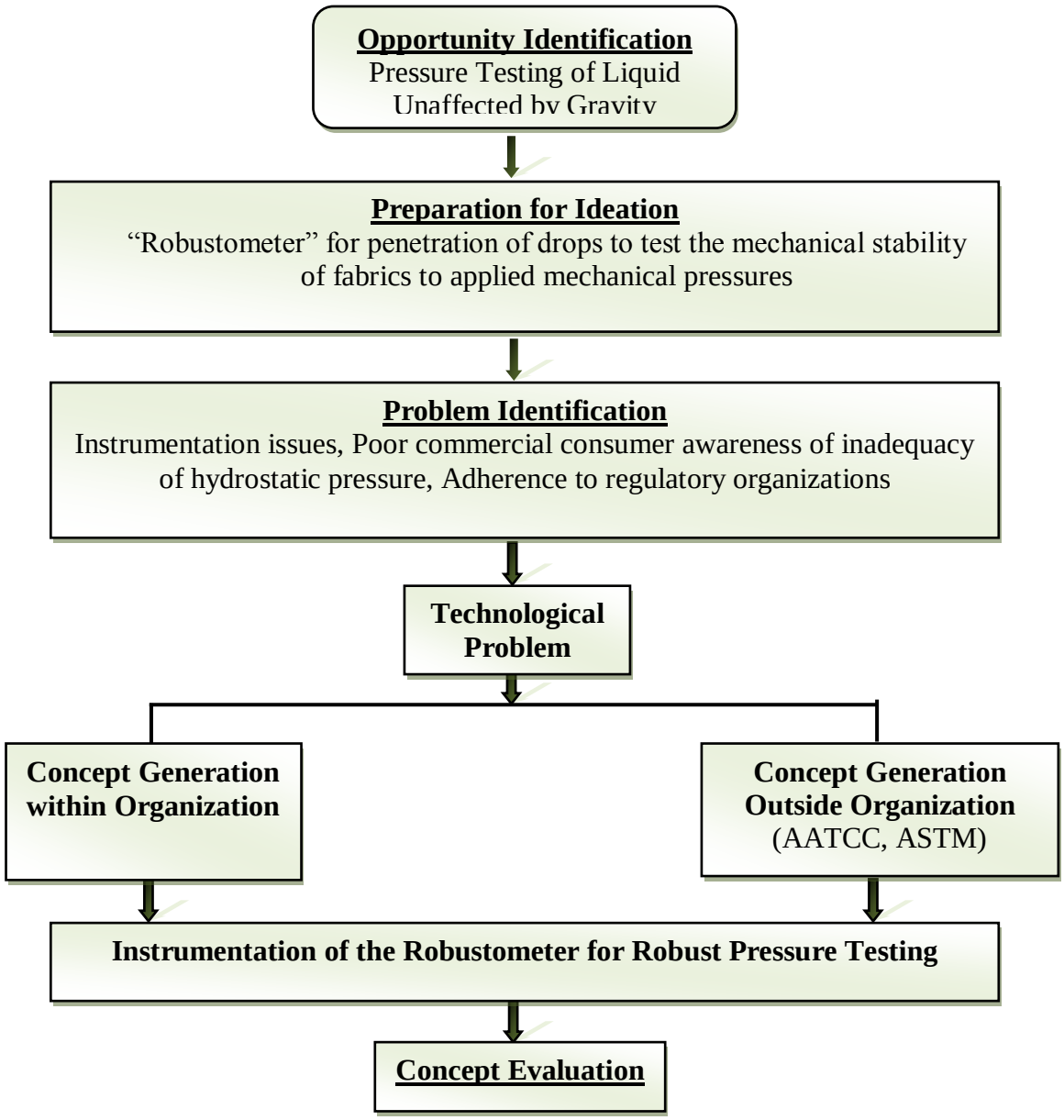

Figure 6.2. Concept generation for "robustometer".

Figure 6.2 depicts concept generation is the part of a project where creative ideas are developed into innovative solutions so as to meet the customer's needs.

Thus, the robustometer and the testing of fabric behavior under application of robust pressure could be feasible for barrier textile materials used in chemical-biological warfare, surgery, pesticide application, etc which are required to protect against small volume penetration of toxic chemicals.

REFERENCES

1. Barthlott, W.; Neinhuis, C., Purity of the sacred lotus, or escape from contamination in biological surfaces. *Planta* **1997,** *202* (1), 1-8.

2. Tavana, H.; Amirafazli,A.; Neumann,A., Fabrication of Superhydrophobic Surfaces of n- Hexatriacontane. *Langmuir* **2006,** *22* (13), 5556-5559.

3. Zhang, X. S., F.; Niu, J.; Jiang, Y.; Wang, Z., Superhydrophobic Surfaces: From Structural Control to Functional Application. *Journal of Materials Chemistry* **2008,** *18,* 621 - 633.

4. Lee, H. J.; Owen, J., Motion of Liquid Droplets on a Superhydrophobic Oleophobic Surface. *Journal of Material Science* **2010,** *46* (1), 69-76.

5. Michielsen, S. L.; Lee, H. J., Design of a Superhydrophobic Surface Using Woven Structures. *Langmuir* **2007,** *23,* 6004-6010.

6. Satam, D., Lee, H., Wilusz, E, An Approach to Mass Customization of Military Uniforms Utilizing Superoleophobic Nonwoven Fabrics. *AATCC Review* **2010,** *59*.

7. Wenzel, R., Resistance of Solid Surfaces to Wetting by Water. *Industrial Eng. Chem* **1936,** *28,* 988-944.

8. Cassie, A.; Baxter, S., Wettability of Porous Surfaces. *Trans. Faraday Society* **1944,** *40,* 546-555.

9. Marmur, A., Wetting on Hydrophobic Rough Surfaces: To Be Heterogeneous or Not To Be? . *Langmuir* **2003,** *19* (20), 8343-8348.

10. Nosonovsky, M.; Bhushan, B., *Multiscale dissipative mechanisms and hierarchical surfaces: friction, superhydrophobicity, and biomimetics*. Springer: Berlin 2008.

11. (a) Bhushan, B.; Nosonovsky, M., Hydrophobic Surface with Geometric Roughness Pattern. 2004; (b) Erbil, H. Y., *Surface chemistry of solid and liquid interfaces*. Blackwell Pub: Oxford, UK, 2006.

12. Sharfrin, E.; Zisman, W. A., Constitutive relations in the wetting of low energy surfaces and the theory of the retraction method of preparing monolayers. *The Journal of Physical Chemistry* **1960,** *64* (5), 519-524.

13. Kovats, E., Wetting of low energy model surfaces. *Pure and Applied Chemistry* **1989),** *61* (11), 1937-1944.

14. Lee, H. J.; Michielsen, S., Lotus Effect: Superhydrophobicity. *Journal of the Textile Institute* **2006,** *97* (455), 455-462.

15. Pal, S.; Weiss, H.; Keller, H.; Müller-Plathe, F., Effect of Nanostructure on the Properties of Water at the Water-Hydrophobic Interface: A Molecular Dynamics Simulation. *Langmuir* **2005,** *21*, 3699-3709.

16. Alberti, G.; DeSimone, A., Wetting of Rough Surfaces: A Homogenization Approach. *Proceedings of the Royal Society A, London* **2004,** *461*, 79-97.

17. Li, W.; Amirfazli, A., A Thermodynamic Approach for Determining the Contact Angle Hysteresis for Superhydrophobic Surfaces. *Journal of Colloid and Interface Science* **2005,** *291* (1), 195-201.

18. Yoshimitsu, Z.; Nakajima, A.; Watanabe, T.; Hashimoto, K., Effects of Surface Structure on the Hydrophobicity and Sliding Behavior of Water Droplets. *Langmuir* **2002,** *18* (15), 5818-5822.

19. Lee, H. J., Design of Artificial Lotus Leaves Using Nonwoven Fabric. *Journal of Material Science* **2009,** *44*, 4645-4652.

20. Tuteja, A.; Choi, W.; Ma, M.; Mabry, J. M.; Mazzella, S. A.; Rutledge, G. C.; McKinley, G.; Cohen, R., Designing Superoleophobic Surfaces. *Science* **2007,** *318* (5856), 1618-1622.

21. Patankar, N. A., Transition between Superhydrophobic States on Rough Surfaces. *Langmuir* **2004,** *20* (17), 7097-7102.

22. Bico, J.; Thiele, U.; Quéré, D., Wetting of textured surfaces. *Colloids and Surfaces: A Physicochemical and Engineering Aspects* **2002,** *206* (1-3), 41-46.

23. Patankar, N. A., Mimicking the Lotus Effect: Influence of Double Roughness Structures and Slender Pillars. *Langmuir* **2004,** *20* (19), 8209-8213.

24. Chen, W.; Fadeev, A.F.; Hsieh, M.C.; Öner, D.; Youngblood; McCarthy, T.J., Ultrahydrophobic and Ultralyophobic Surfaces: Some Comments and Examples *Langmuir* **1999,** *15* (10), 3395-3399.

25. Koishi, T.; Yasuoka, K.; Fujikawa, S.; Ebisuzak, T.; Zenge, X.C., Coexistence and Transition Between Cassie and Wenzel State on Pillared Hydrophobic Surface. *PNAS* **2009,** *106* (21), 8435–8440.

26. Shuttleworth, R.; Bailey, G., The Spreading of Liquid Over a Rigid Solid. Discuss. . *Faraday Society* **1948,** *3*, 16-22.

27. Johnson, R.; Dettre, R., Contact Angle Hysteresis, in Contact Angle, Wettability, and Adhesion. *Advances in Chemistry* **1964,** *43*, 112-135.

28. Lafuma, A.; Quéré, D., Superhydrophobic States *Nature Materials* **2003,** *2*, 457-460.

29. Patankar, N. A., On the Modeling of Hydrophobic Contact Angles on Rough Surfaces. *Langmuir* **2003,** *19* (4), 1249-1253.

30. Extrand, C., Model for Contact Angles and Hysteresis on Rough and Ultraphobic Surfaces. *Langmuir* **2002,** *18* (21), 7991-7999.

31. Sun, M. L., C.; Xu, L.; Ji, H.; Ouyang, Q.; Yu, D.; et al. , Artificial Lotus Leaf by Nanocasting. *Langmuir* **2005,** *21* (19), 8978-8981.

32. Herminghaus, S., Roughness-induced non-wetting. *Europhysics Letters* **2000,** *52*, 165.

33. Shibuichi, S.; Onda, T.; Satoh, N.; Tsujii, K., Super Water-Repellent Surfaces Resulting from Fractal Structure *The Journal of Physics Chemistry* **1996,** *100* (50), 19512-19517.

34. Bico, J. M., C.; Quéré, D., Pearl Drops. *Europhysics Letters* **1999,** *47*, 220–226.

35. Burton, Z.; Bhushan, B., Hydrophobicity, Adhesion, and Friction Properties of Nanopatterned Polymers and Scale Dependence for Micro- and Nanoelectromechanical Systems. *Nano Letters* **2005,** *5* (8), 1607-1613.

36. (a) Jung, Y.; Bhushan, B, Wetting behaviour during evaporation and condensation of water microdroplets on superhydrophobic patterned surfaces *Journal of Microscopy* **2006,** *229* (1), 127-140; (b) Jung, Y.; Bhushan, B., Micro- and nanoscale characterization of hydrophobic and hydrophilic leaf surfaces. *Nanotechnology* **2006,** *17* (11).

37. Neinhuis, C.; Barthlott, W., Characterization and Distribution of Water-Repellent, Self-Cleaning Plant Surfaces. *Annals of Botany* **1997,** *79*, 667-677.

38. In *http://images.iop.org/objects/phw/news/9/4/3/0504031.jpg, http://www.technex.co.jp/tinycafe/lecture03/m-c2.jpg, http://api.ning.com/files/*, 2011.

39. Baker, E., *Chemistry and Morphology of Plant Epicuticular Waxes*. CE Price: New York 1982.

40. Gao, L.; McCarthy, T. J., Teflon is Hydrophilic. Comments on Definitions of Hydrophobic, Shear versus Tensile Hydrophobicity, and Wettability Characterization. *Langmuir* **2008,** *24* (17), 9183-9188.

41. (a) He, B.; Patankar, N. A.; Lee, J, Multiple Equilibrium Droplet Shapes and Design Criterion for Rough Hydrophobic Surfaces. *Langmuir* **2003,** *19* (12), 4999-5003; (b) Kijlstra, J.; Reihs, K.; Klami, A., Roughness and topology of ultra-hydrophobic surfaces. *Colloids and Surfaces A: Physicochemical and Engineering Aspects* **2002,** *206*, 521 - 529; (c) Shibuichia, S.; Yamamotoa, T.; Ondab, T.; Tsujii, K., Super Water- and Oil-Repellent Surfaces Resulting from Fractal Structure. *Journal of Colloid and Interface Science* **1998,** *208* (1), 287-294.

42. Hayn, R. A.; Owen, J. R.; Boyer, S. A.; McDonald, R. S.; Lee, H. J. , Preparation of highly hydrophobic and oleophobic textile surfaces using microwave-promoted silane coupling. *Journal of Materials Science* **2010**, 1-7.

43. Ohkubo, Y. T., I.; Onishi, S.; Ogawa, K., Preparation and Characterization of Super-hydrophobic and Oleophobic Surface. . *Journal of Materials Science* **2009,** *45* (18), 4963-4969.

44. Cao, L.; Price, T. P.; Weiss, M.; Gao, D., Super Water- and Oil-Repellent Surfaces on Intrinsically Hydrophilic and Oleophilic Porous Silicon Films. *Langmuir* **2008,** *24* (5), 1640-1643.

45. Liu, M. W., S.; Wei, Z.; Song, Y.; Jiang, L., Bioinspired Design of a Superoleophobic and Low Adhesive Water/Solid Interface *Advanced Materials* **2009,** *21* (6), 665-669.

46. Im, M.; Im, H.; Lee, J.; Yoon, J.; Choi, Y., A Robust Superhydrophobic and Superoleophobic Surface with Inverse-Trapezoidal Microstructures on a Large Transparent Flexible Substrate. *Soft Matter* **2010,** *6* 1401-1404.

47. Extrand, C., Designing for Optimum Liquid Repellency. *Langmuir* **2006,** *22* (4), 1711-1714.

48. Tuteja, A.; Choi, W.; Mabry, J.M.; McKinley, G.; Cohen, R., Robust Omniphobic Surfaces. *PNAS* **2008,** *105* (47), 18200-18205.

49. Tuteja, A.; Choi, W.; Mckinley, G.; Cohen, R.; Mabry, J., Washington, DC: Tunable Surface. **2010**.

50. Chhatre, S. S.; Choi, W.; Tuteja, A.; Park, K.; Mabry, J. M.; McKinley, G. H., Scale Dependence of Omniphobic Mesh Surfaces. *Langmuir* **2009,** *26* (6), 4027-4035.

51. Cao, H.; Hu. H.; D. Gao., Design and fabrication of microtextures for inducing a super-hydrophobic behavior on hydrophilic materials. *Langmuir* **2007,** *23* (4310-4314).

52. Ahuja, A. T., J. A.; Lifton, V.; Sidorenko, A. A.; Salamon, T. R.; Lobaton, E. J.; Kolodner, P.; Krupenkin, T. N. , Nanonails: A Simple Geometrical Approach to Electrically Tunable Superlyophobic Surfaces. *Langmuir* **2008,** *24*, 9-14.

53. Kwon Y.; Patankar N.A.; Choi J.; Lee J., Design of Surface Hierarchy for Extreme Hydrophobicity. *Langmuir* **2009,** *25* (11), 6129-6136.

54. Vagharchakian, L.; Restagno, F.; Leger. L., Capillary Bridge Formation and Breakage: A Test to Characterize Antiadhesive Surfaces. *J. Phys. Chem. B* **2009,** *113* (12), 3769-3775.

55. Michielsen, S., The Effect of Grafted Polymeric Lubricant Molecular Weight on the Frictional Characteristics of Nylon 6,6 Fibers. *Journal of Applied Polymer Science* **1999,** *73* (1), 129–136.

56. Reyssat, M.; Yeomans., J.M.; Quéré, D., Impalement of Fakir Drops. *Europhys. Lett.* **2008,** *26006*.

57. Adamson, A. W., *Physical chemistry of surfaces (5. ed.)*. Wiley: New York, 1990.

58. Raheel, M., *Modern Textile Characterization Methods*. Marcel Dekker: New York, 1996.

59. AATCC Technical Manual, A. A. o. T. a. C., In *73*, Research TrianglePark, NC, 1998; pp 253-254, 186-188, 206-207

60. Newburgh, L. H., *Clothing test methods* Edward Brothers Inc.: Washington, D.C 1945.

61. Fan, Q., *Chemical testing of textiles*. Woodhead Pub: Cambridge, 2005.

62. International, A., ASTM F1670 Standard Test Method for Resistance of Materials Used in Protective Clothing to Penetration by Synthetic Blood. West Conshohocken, PA, 2008.

63. International, A., ASTM F903 Standard Test Method for Resistance of Materials Used in Protective Clothing to Penetration by Liquids. West Conshohocken, PA, 2010.

64. McCullough, E.A.; Johnson, P.W.; Shim, H., In *A Comparison of ASTM F1670 and F 1819 Standards for Measuring the Barrier Properties of Protective Clothing Using Syntheitc Blood. Performance of Protective Clothing: Issues and Priorities for the 21st Century and Materials.*, Nelson, C. N. H., N.W., Ed. ASTM STP 1386: **2000**.

65. Huang, W.; Leonas, K, Evaluating a One-Bath Process for Imparting Antimicrobial Activity and Repellency to Nonwoven Surgical Gown Fabrics. *Textile Research Journal* **2000,** *70* (9), 774-782.